Spring 2018

# DESIGN IMPROVEMENTS TO SULFATE-REDUCING BIOREACTORS FOR MINE-INFLUENCED STREAM REMEDIATION IN COLD CLIMATES

Katrina Moreira
*Montana Tech*

# DESIGN IMPROVEMENTS TO SULFATE-REDUCING BIOREACTORS FOR MINE-INFLUENCED STREAM REMEDIATION IN COLD CLIMATES

by

Katrina Elizabeth Moreira

A thesis submitted in partial fulfillment of the
requirements for the degree of

Master of Science in Environmental Engineering

Montana Tech

2018

## Abstract

Mine-influenced water (MIW), a waste water product containing heavy metals and sulfates, is a significant pollution source to waters in Montana. Implementing a low cost, passive treatment system, such as a sulfate-reducing bioreactor (SRBR), is desired for remediation of streams influenced by heavy metals in remote locations. SRBR systems operate by using organic matter and sulfate-rich water to precipitate and immobilize dissolved heavy metals. Sulfate-reducing bacteria utilize the organic matter as an electron donor to convert sulfate to sulfide, and then sulfide in the bioreactor is utilized to precipitate heavy metals. Under ideal operating conditions, SRBR systems can remove >98% of dissolved heavy metals. However, heavy metal removal efficiency is compromised by cold climates, acidic conditions, impaired hydraulic conductivity and introducing oxygen into the system. Previous published studies have research design modifications to improve SRBRs to overcome these operating challenges. These modifications included adding a liquid carbon source, limestone and adsorbents. Physical adsorption is a reversible process, and therefore has potential to supplement SRBR systems throughout inhibited performance during winter months with continued regeneration in the summer time, and permit further reuse. This research investigated design enhancements to SRBR systems to improve winter-time heavy metal treatment using an adsorbent material with the intent to apply this technology to an impaired stream in Butte, MT, Grove Gulch, which is affected by mine tailing in the water shed along its banks.

Experiments were carried out to characterize temperature effects on SRBR systems, examine isolated adsorption-desorption effects, and apply adsorbent materials within an SRBR to quantify the extent of heavy metal removal under cold temperature conditions. Initially, batch experiments in flasks were carried out to assess the ability for adsorption of heavy metals to an adsorbent, followed by desorption and precipitation of heavy metals allowing for reuse of the adsorbent. Batch desorption experiments were variable, yet demonstrated potential for regeneration of the selected adsorbent, granular activated carbon (GAC). Desorption and precipitation of copper and zinc varied from 14-91%. The investigated bench-scale SRBR removed >98% of influent copper and zinc ions operating under summer-time conditions (22°C). Winter-time operating conditions (5°C) resulted in decreased removal efficiencies of copper (88-99.98%) and zinc (52-99.91%). The success of this project determined that SRBR systems have the potential to adequately operate in a cold climate region, such as Butte, MT, using a supplementary adsorbent material. Heavy metal removal in the SRBR using GAC to supplement the reactor under winter-time conditions was 85-99%. Microbial activity was hindered while influenced by winter-time operating conditions, but did not diminish. Research findings revealed the potential for adsorption of heavy metals during winter-time conditions, followed by desorption and precipitation during summer months. The discoveries of this thesis raised further potential research questions and recommendations for full-scale operation.


Keywords: Sulfate Reducing Bioreactor, Mine Influenced Water, Cold Climate, Remediation, Granular Activated Carbon, Adsorption, Desorption, Adsorbent Regeneration

## Dedication

I would like to dedicate this work to my boyfriend, Alex, for all his love, support and encouragement. I would also like to thank my friends and family for their continued moral support. A special thank you to Dave and Jayne Meleshko who made getting my master's degree possible, and for their invaluable mentorship and guidance.

## Acknowledgements

I would like to thank the following people who made this project possible with their continued guidance and support throughout the research and laboratory work that went into this project:

**Dr. Raja Nagisetty****
Montana Tech of the University of Montana – Department of Environmental Engineering

**Dr. Bill Drury***
Montana Tech of the University of Montana – Retired Faculty of the Department of Environmental Engineering

**Dr. Christopher Gammons***
Montana Tech of the University of Montana – Department of Geological Engineering

**Jeanne Larson***
Montana Tech of the University of Montana – Department of Environmental Engineering

**Robert Roll***
Montana Department of Environmental Quality – State Superfund Section

**Gary Wyss**
Montana Tech of the University of Montana – Center for Advanced Mineral and Metallurgical Processing

**Dr. Kumar Ganesan**
Montana Tech of the University of Montana – Department of Environmental Engineering

**Matt Strozewski**
Montana Tech of the University of Montana – Graduate Student, Department of Environmental Engineering

***Committee Member**

****Committee Chair**

# Table of Contents

## List of Tables

## List of Figures

## List of Equations

Equation

## Glossary of Terms and Acronyms

| Term | Definition |
|---|---|
| Adsorbate | Aqueous media containing dilute mine-influenced water for adsorption |
| Adsorbent | Material to adsorb heavy metals |
| Adsorption | Adhesion of adsorbate to an adsorbent material |
| ALD | Anoxic Limestone Drain |
| AMD | Acid Mine Drainage |
| ARCO | Atlantic Richfield Company |
| Batch | Experiments performed inside an isolated flask |
| BSR | Bacterial Sulfate Reduction |
| Breakthrough | Complete saturation of adsorption sites on the adsorbent |
| CMRC | Copper Mountain Recreation Complex |
| DI | Deionized |
| Desorption | Reversal of adsorption of adsorbate on an adsorbent |
| Effluent | Water exiting a reactor system |
| GAC | Granular Activated Carbon |
| ICP-OES | Inductively-Coupled Plasma Optical Emission Spectrometer |
| Influent | Water entering a reactor system |
| MIW | Mine-Influenced Water |
| MDL | Minimum Detection Limit |
| MTDEQ | Montana Department of Environmental Quality |
| PAC | Powdered Activated Carbon |
| SEM | Scanning Electron Microscope |
| SRBR | Sulfate-Reducing Bioreactor |
| USEPA | United States Environmental Protection Agency |

# 1. Introduction

## 1.1. History

Hard rock mining was a significant historical contributor to economic development in Montana (Montana Department of Labor & Industry, 2014). Heavy metals are a significant pollution source to waters in Montana resultant of nearly 150 years of extensive mining operations (Duaime, et al. 1995; Gammons et al., 2005). Mine-influenced water (MIW) is defined as any form of water impacted by mining operations (United States Environmental Protection Agency [USEPA], 2014). When attributed to the hard rock mining process, heavy metals can enter waterbodies by means of acid mine drainage (AMD), or by dissolution through mine tailings and waste rock (Akcil & Koldas, 2006; Gammons et al., 2005). Across the United States, over 10,000 miles of streams and water bodies are impacted by MIW (Akcil & Koldas, 2006). Consequently, there are detrimental effects to human health and aquatic life when streams are influenced by heavy metals in exceedance of regulatory thresholds (USEPA, 2014).

Heavy metals contained in waste sulfide mineral tailings become particularly mobile when exposed to water and oxygen (Lindsay et al., 2015). Ore waste rock and tailings contain high concentrations of numerous toxic heavy metals, such as copper, nickel, zinc and lead. Mobility of heavy metals in waste tailings are controlled by chemical and biological mechanisms. As tailings and waste rock weather over time, dissolution of heavy metals can occur by contact with water bodies or storm water. Highly weathered mine tailings can also contribute to dissolution of heavy metals into waters in an anaerobic environment (Ribet et al., 1995).

Throughout the hard rock mining process, acid mine drainage (AMD) is created by oxidation of sulfide minerals, resulting in acidic, sulfate and heavy metal rich water flowing from

the mine itself (Cohen, 2006; Stumm & Morgan, 1981). The generic equation of AMD generation that begins the cycle of oxidation is shown in Eqn. (1) (Stumm & Morgan, 1981). Further acidity and oxidation of ferrous iron to ferric iron can be facilitated by iron oxidizing bacteria. Ferric iron continues to oxidize pyrite, resulting in further generation of AMD. In addition to iron, other metals, such as copper, zinc, lead and arsenic, are released with AMD (Cohen, 2006).

$$FeS_2 + 7/2\ O_2 + H_2O \rightarrow Fe^{2+} + 2SO_4^{2-} + 2H^+ \quad (1)$$

## 1.2. Grove Gulch

Within the Silver Bow Creek/Butte Superfund site, it is estimated 26 miles of stream and streamside habitat have been impacted by MIW (USEPA, 2016). Remedial actions have been performed; including removing and capping tailings. Despite remedial efforts, extensive heavy metal contamination in the Butte, MT area persists. Grove Gulch is a 7.6-mile long stream located southwest of Butte and flowing northeast joining Blacktail Creek in the city limits of Butte. Extensive heavy metal contamination has been quantified in Grove Gulch as the stream enters Butte (Craig, 2016). Specifically, dissolved zinc concentrations in the waters of Grove Gulch are as elevated as 7168 µg/L, as confirmed in August 2015 (Figure 1). Among other heavy metals of concern in Grove Gulch, elevated zinc concentrations exceed Circular DEQ-7 acute and chronic water quality standards of 37.0 µg/L at 25 mg/L hardness (Craig, 2016; Montana Department of Environmental Quality [MTDEQ], 2012).

Sources of heavy metal contamination in Grove Gulch have been attributed to the dissolution of heavy metals by waste rock and tailings deposited along stream beds (Craig, 2016). In 1914, the Timber Butte Zinc Mill was constructed and formerly processed 450 tonnes per day of zinc-rich ore attained from the Elm Orlu Mine. The tailings generated by the

Timber Butte Zinc Mill were known as the Clark Tailings, and were never removed from the site. The Clark Tailings introduced extensive heavy metal contamination in the area formerly known as the Timber Butte Zinc Mill. Currently, the Copper Mountain Recreation Complex (CMRC) lies above the location of the former Timber Butte Zinc Mill. Grove Gulch flows in a pipe beneath the CMRC prior to flowing into Blacktail Creek.

Another identified contributor to heavy metal contamination in Grove Gulch is by dissolution with the Colorado tailings (Craig, 2016). The Colorado tailings were generated by the Colorado Smelter and Butte Reduction Works, and were disposed of along the streamside of Silver Bow Creek (Craig, 2016). The Colorado tailings were rich in copper, zinc and lead, and contributed extensive heavy metal contamination to Silver Bow Creek (Duaime et al., 1985). Prior to constructing the CMRC, the Old Butte Municipal Landfill was established on the same property as the former Timber Butte Zinc Mill (Craig, 2016). The Colorado tailings were moved to this landfill in 1998, alongside the Clark Tailings, and capped using clean soil (Craig, 2016; USEPA, 2006). At that time, Atlantic Richfield Company (ARCO) constructed the CMRC over the capped Clark and Colorado tailings.

As a result of extensive heavy metal contamination in both the sediments and waters of Grove Gulch, best management practices were developed (Craig, 2016). The recommended remedial actions to remove heavy metal contamination were implementing vegetated stream buffers and a subsurface sulfate-reducing bioreactor (Craig, 2016).

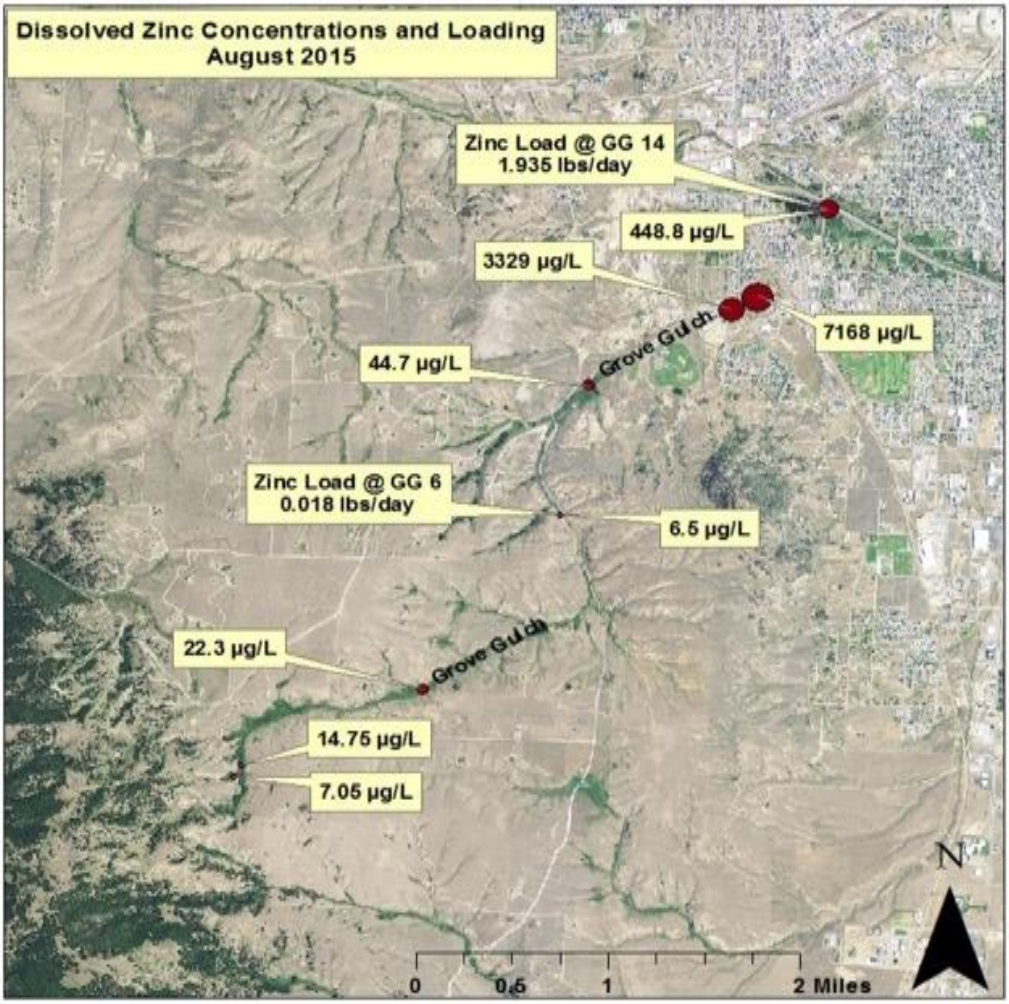


**Figure 1: August 2015 dissolved zinc concentrations and loadings in Grove Gulch (Craig, 2016).**

## 1.3. Treatment Technologies

Recommended treatment technologies for MIW include active and passive treatment technologies. Suggested active technologies include lime precipitation, reverse osmosis, ion exchange, and fluidized bed reactors (USEPA, 2014). Active technologies typically require ongoing maintenance and energy requirements. Passive treatment technologies utilize gravity-driven flow regimes and natural constituents, such as woodchips and rocks, and require minimal maintenance (USEPA, 2014). Passive technologies are preferred by regulatory bodies, such as

the USEPA. The feasibility of implementing active technologies in remote locations can be limited, as well as energy intensive and costly.

Currently implemented passive treatment technologies for remediation of MIW are phytoremediation, constructed wetlands and biochemical reactors (USEPA, 2014). These technologies have limitations. A challenge associated with phytoremediation is the limitation to the depth of the roots for heavy metal uptake. Alternatively, the combination of a constructed wetland and biochemical reactor has great potential for a passive, cost effective solution requiring minimal maintenance and providing long-lasting effects (Gammons & Frandsen, 2001). Sulfate-reducing bioreactors (SRBR) are a well-researched and successfully implemented passive technological approach for treatment of MIW (Drury, 1999; Dvorak et al., 1992; Gammons & Frandsen, 2001; USEPA, 2015).

## 1.4. Sulfate-Reducing Bioreactors (SRBRs)

SRBRs are a cost-effective, passive approach to mitigate and treat contaminated sites impacted by MIW (Cohen, 2006; Gammons & Frandsen, 2001). Implementation of passive SRBRs have proven to be successful at full scales of operation at mine sites (Table I). The passive biological treatment approach provides cost saving benefits and lower system maintenance requirements (Cohen, 2006). There are no ongoing waste management requirements associated with SRBRs, since waste metal sulfides are contained inside the bioreactor. Although, SRBRs eventually clog and require rebuilding (Tsukamoto et al., 2004).

**Table I: Full-scale SRBRs implemented at mine sites in South Carolina, Missouri, Wyoming and Pennsylvania and corresponding heavy metal removal.**

| Location | Percent Heavy Metal Removal | Reference |
|---|---|---|
| Brewer Gold Mine, South Carolina | Copper, zinc, aluminum and iron: 95-100% | (Gusek, 2000) |
| Doe Run Company, West Fork Unit, Missouri | Lead: 90-95% | (Gusek, 2000) |
| Eagle Mine, Minturn, CO | Arsenic, chromium, cadmium, copper, iron, lead and zinc: 99-100% | (Cohen, 2006) |
| Ferris-Haggarty Mine, Wyoming (-4°C to 4°C) | Copper: 65-99% | (Gusek, 2000) |
| Fran Mine, Pennsylvania | Aluminum: 99.7-99.9%<br>Iron: 87-99% | (Gusek & Wildeman, 2002) |

The design of an SRBR system can be characterized as a packed bed reactor, employing either lateral or upwards flow (Dev et al., 2017; Gusek, 2004). In a packed bed reactor, water treatment is facilitated using fixed, solid media (Crittenden et al., 2012). Water entering the reactor is defined as the influent (or inflow), and water exiting the reactor is the effluent (or outflow). Once water is flowing within the solid media, pollutant removal can be achieved via a chemical reaction. An example of an upflow packed bed reactor is shown in Figure 2 (Crittenden et al., 2012).

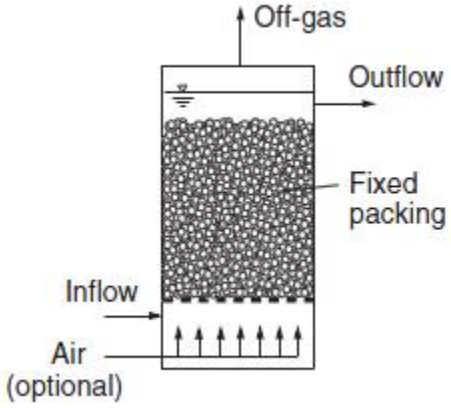


**Figure 2: Packed bed reactor design employing upward flow (Crittenden et al., 2012).**

Employing the design of a packed bed reactor, the solid media used to facilitate a biochemical reaction in SRBRs can consist of woodchips, manure, hay, or waste dairy products (Cohen, 2006; Drury, 1999; Gusek, 2004; USEPA, 2015). It is common to add gravel to optimize flow within the bioreactor (Cohen, 2006). Limestone is often added to promote conditions of alkalinity (Cohen, 2006; Gusek, 2004; Neculita et al., 2007). A full-scale SRBR implemented in Eagle Mine, Minturn, CO is shown as a schematic cross-section in Figure 3, where a perforated pipe immersed with gravel is used to distribute flow upwards through a mixed substrate of manure, hay, woodchips and limestone (Cohen, 2006).

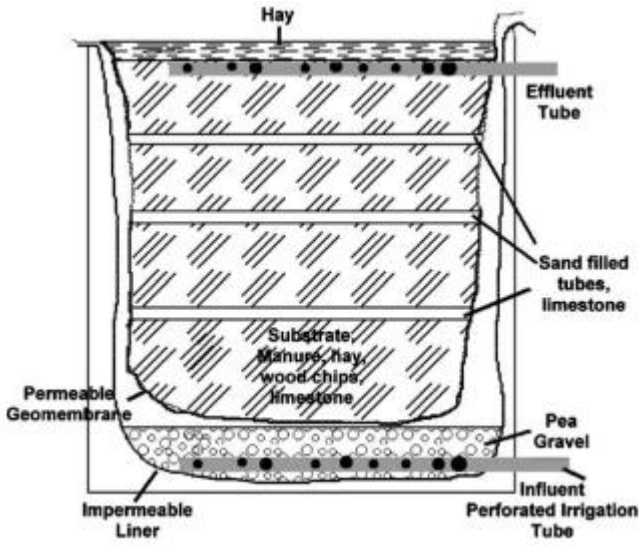


**Figure 3: Full-scale SRBR schematic implemented in Eagle Mine, Minturn, CO (Cohen, 2006).**

### 1.4.1. Bacterial Sulfate Reduction

Heavy metal removal in SRBR systems is predominantly attributed to biologically mediated bacterial sulfate reduction (BSR) (Drury, 1999). Sulfate-reducing bacteria (*Desulfovibrio sp*.) thrive and populate by utilizing sulfate ions and simple organic compounds. Complex organic compounds, such as woodchips, degrade into simple organic compounds, which is represented as $CH_2O$. Simple organic compounds serve as an electron donor and are

oxidized (Dvorak et al., 1992). As a result, sulfate-reducing bacteria convert sulfate ions to sulfide ion species, and the organic electron donor is converted to bicarbonate ions (Eqn. 2)

$$SO_4^{2-} + 2CH_2O \rightarrow H_2S + 2HCO_3^- \quad (2)$$

The pH of the MIW entering the SRBR determines which sulfide species will dominate the equilibrium (Eqn. 3) (Cohen, 2006). Low pH conditions result in gaseous $H_2S$ species. At a neutral pH, dissolved $HS^-$ and $H_2S$ are dominant in the system. High pH conditions shift the equilibrium to produce predominantly $S^{2-}$.

$$H_2S \rightleftharpoons HS^- + H^+ \rightleftharpoons S^{2-} + 2H^+ \quad (3)$$

The dominant species of sulfide in the SRBR readily precipitates dissolved heavy metals to insoluble metal sulfides, with hydrogen ions as a byproduct (Eqn. 4).

$$H_2S + Me^{2+} \rightarrow MeS\,(s) + 2H^+ \quad (4)$$

Hydrogen ions are consumed by alkalinity produced by BSR or an anoxic limestone drain supplementing the SRBR. The net reaction of heavy metal precipitation by BSR is shown in (Eqn. 5).

$$SO_4^{2-} + Me^{2+} + 2CH_2O \rightarrow MeS\,(s) + 2H_2CO_3 \quad (5)$$

### 1.4.2. Ideal Performance

When functioning under ideal conditions, passive SRBR systems yield desirable removal of aqueous heavy metal ions (Willow & Cohen, 2003). Upwards of 98% heavy metal removal efficiency is observed when BSR is facilitated in an appropriate environment. Ideal conditions are upheld in full-scale passive SRBR systems with adequate hydraulic conductivity, continuous subsurface flow, neutral pH, moderate to warm temperature, available organic carbon, and anaerobic conditions (Gammons & Frandsen, 2001; Gusek, 2004).

### 1.4.3. Limitations

#### 1.4.3.1. Cold Climate

Introducing cold temperature conditions to a passive SRBR system results in a significant decrease in rates of organic matter degradation and bacterial growth rates (Drury, 2000; Machemer & Wildeman, 1992). Modelled SRBR performance at 1°C returned considerably lower sulfate reduction outputs (Drury, 2000). Increasing hydraulic retention time mitigates decreased sulfate reduction rates, but is not always an option when treatment demands must be met (Drury, 2000). The solubility of hydrogen sulfide in water increases with decreasing temperature, which is a benefit to SRBR systems when sulfate reduction declines (Neculita et al., 2007). Sulfate-reducing bacteria can tolerate temperature conditions between -5°C to 75°C (Neculita et al., 2007; Postgate, 1984). Sulfate removal in a bench-scale SRBR system at 6°C was observed at <2% without supplements (Tsukamoto et al., 2004).

#### 1.4.3.2. Influence of pH

When pH conditions deviate from 5 to 8, BSR declines and this negatively affects heavy metal removal in SRBR systems (Brown et al., 1973; Willow & Cohen, 2003). BSR is most adversely impacted by acidic pH when compared to other limitations that may inhibit microbial activity (Willow & Cohen, 2003). Excess protons reduce the availability of electron donors, as well as mobilize hydrogen sulfide in the gaseous phase (Cohen, 2006; Willow & Cohen, 2003). Acidic pH conditions are less favorable towards metal sulfide precipitation. When influent water is acidic, an anoxic limestone drain (ALD) may adjust the pH above 5 (USEPA, 2015).

#### 1.4.3.3. Aerobic Conditions

Sulfate-reducing bacteria are anaerobes and populations fail to thrive under aerobic conditions (Brown et al., 1973; Willow & Cohen, 2003). Dissolved oxygen content in the water

entering the reactor is of less importance than the substrate composition to facilitate BSR (Willow & Cohen, 2003). A high organic carbon content in the substrate allows anaerobic conditions to be maintained (Neculita et al., 2007). Once the water contacts the organic substrate, the requirement for an anaerobic environment is satisfied.

#### 1.4.3.4. Hydraulics

Hydraulic residence time depends on substrate permeability, reactor volume, and the influent flow rate (Dvorak et al., 1992). Hydraulic residence time that is too short leads to lowered production of alkalinity. Alternatively, an excessively long hydraulic residence time leads to excess hydrogen sulfide and alkalinity production exiting the system for heavy metal precipitation.

Plugging of reactors are among the most common reasons of failures in efficiency (Tsukamoto et al., 2004). Maintenance of adequate hydraulic conductivity is best achieved using a substrate combination of wood and rocks for sufficient pore space and connectivity. Manure composts in SRBRs are known to clog more readily than wood-based substrates (Tsukamoto et al., 2004). Clogging can also occur when the flow distribution in the reactor is uneven, resulting in spaces with dead volume (Gusek, 2004). Dead volume in a reactor also results in lower sulfate reduction rates, since there are unused volumes of substrate (Crittenden et al., 2012).

#### 1.4.3.5. Suspended Solids

When the flow rate exiting the SRBR is too fast, metal sulfide particles are carried away from the reactor (Dvorak et al., 1992). Once heavy metal particles escape the bioreactor, there is potential for heavy metals to re-enter a stream by re-oxidation and dissolution (Gammons & Frandsen, 2001). As a result, it is important to monitor both total recoverable metals and total dissolved metals (Gammons et al., 2000; Gammons & Frandsen, 2001).

### 1.4.4. Design Improvements

#### 1.4.4.1. Liquid Carbon Sources

The addition of readily available electron donors, such as ethanol, methanol or acetate, have proven to be successful in a laboratory setting (Tsukamoto et al., 2004). Addition of ethanol (138 mg/L) in the influent significantly improved cold temperature reactor performance, resulting in >95% removal of iron at 6°C. While an additional electron donor may improve winter-time efficiency, adding a liquid carbon source to the influent brings forth continuous maintenance requirements. The effects of a continuous supplementary carbon source on long-term reactor performance are not known.

#### 1.4.4.2. Anoxic Limestone Drains (ALD)

Limestone is a widely-implemented supplement to SRBR systems (Cohen, 2006; Gusek, 2004). ALDs accomplish buffering of pH in influent water to a neutral range (Cohen, 2006). Some removal of heavy metals using an ALD can occur by metal hydroxide precipitation (USEPA, 2014). ALDs assist in adjusting the pH of acidic influent, as low pH impairs SRBR function (Cohen, 2006).

#### 1.4.4.3. Adsorbents

A prior study investigated cold temperature performance of SRBR systems with the addition of biochar to the substrate and 16 mg/L of ethanol in the influent (Janin & Harrington, 2015). Throughout conditions of 6°C and 3°C operation of an SRBR supplemented with biochar and ethanol, heavy metal removal efficiency showed significant improvement when compared to a control SRBR (no biochar) while continuing to add ethanol to the influent.

When sulfate reduction is at a minimum, dissolved heavy metals adsorb to organic substrate in the SRBR (Machemer & Wildeman, 1992). Once the capacity of adsorption to

woodchips is spent, heavy metals begin to desorb. Adsorption of heavy metals to woodchips during winter operation is limited. Employing adsorption as a secondary mechanism is best achieved using a material with a greater adsorbent capacity (Janin & Harrington, 2015).

## 1.5. Heavy Metal Adsorption

Adsorption is the process in which an adsorbate forms an attraction or bond with the surface of an adsorbent (Crittenden et al., 2012). The solid surface at which adsorption occurs is the adsorbent. The adsorbate is the pollutant molecule adhered to the adsorbent surface. Two mechanisms of adsorption that can occur are chemical or physical adsorption. Chemical adsorption is irreversible, specific and finite, and occurs by reaction of the adsorbate with the adsorbent forming an ionic or covalent bond. Chemical adsorption is limited to a single molecular layer due to the specific nature of the bond with the adsorbate. Physical adsorption is driven by van der Waals attractive forces between the adsorbate and adsorbent surface. Multiple molecular layers can form on the adsorbent by physical adsorption. Physical adsorption is nonspecific, reversible and finite. Nonspecific adsorption allows for multiple molecular layers of adsorption by coulombic attraction. In practice, physical adsorption is more common.

Breakthrough of an adsorbent material occurs when the adsorbate loading is high and all adsorption sites are completely saturated (Crittenden et al., 2012). Once breakthrough of the adsorbent occurs, heavy metals begin to pass the adsorbent and enter the effluent. While adsorption of heavy metals is proven effective, it is costly to continuously replenish an adsorbent material after breakthrough occurs.

### 1.5.1. Adsorbent Regeneration

Regeneration of activated carbon can be achieved by a chemical process using an acid or base reagent to promote desorption (Crittenden et al., 2012; Mugisidi et al., 2007). Although

physical adsorption is a reversible process, activated carbon cannot be regenerated in whole (Crittenden et al., 2012). Generally, regeneration is only useful when chemical reagents can be recycled (Crittenden et al., 2012). Acid reagents leach adsorbed heavy metals physically adsorbed to activated carbon to free adsorption sites for re-use. Desorbed heavy metals using acid reagents are in the dissolved phase when exiting the adsorbent. Base reagents remove physically adsorbed heavy metals by precipitation. Once an adsorbent is regenerated, the material can be reused for adsorption.

## 1.6. Research Elements

The primary goal of this research is to establish the potential for sequestering heavy metals using an adsorbent material during winter months while sulfate reduction is inhibited. Once microbial activity in the SRBR resumes in the summer months, the potential for reuse of an adsorbent by desorption of heavy metals via sulfide precipitation will be investigated.

Specific objectives include:

1. Comparison of adsorbent materials best suited to supplement an SRBR system during cold temperature operation, with emphasis on the potential for reuse by regeneration.
2. Characterization of cold and warm temperature effects on SRBR heavy metal removal efficiency.
3. Determine adsorption-desorption mechanisms of the selected adsorbent under the influence of temperature change in the SRBR.

# 2. Methods

The potential to improve SRBR performance was initially evaluated using batch adsorption and desorption experiments. Following the batch experiments, an adsorbent material was added to a bench-scale SRBR.

## 2.1. Batch Adsorption and Desorption Experiments

A total of six Trials were performed for the batch adsorption-desorption experiments using GAC. A single Trial was conducted using natural coconut coir fibers (NF). A batch experiment refers to Trials of adsorption and desorption performed inside of a flask. The procedure was followed for Trials 4-6 as described in Methods sections 2.1.2 to 2.1.5. Refer to Table II for differences in procedure followed throughout each of the Trials. Changes to further trial batch experiments were implemented for Trials 4-6 as required.

### 2.1.1. Methods Development

It was during the first trial that the importance of the powdered activated carbon (PAC) that was mixed with GAC was discovered. There was an apparent selectivity of adsorption of heavy metals onto PAC that was mixed among GAC. After 7 days of adsorption, a syringe was used to draw a sample of adsorbate. The adsorbate matrix contained metals adsorbed to PAC and remaining dissolved heavy metals. The suspended PAC in the adsorbate caused a remarkable interference. Due to the interference of PAC, meaningful results could not be interpreted from the first trial, and future trials were modified based on these findings.

Trials 2-3 were modified so that GAC were sieved, rinsed and soaked with DI water prior to beginning any adsorption experiments. Adsorption occurred over 24 hours at 5°C and desorption occurred over 24 hours at 22°C. Efforts were made to remove as much PAC as possible prior to adsorption. The experiments were conducted in triplicate with three flasks

concurrently. In the process of preparing heavy metal samples, the third flask was compromised. Results for this set of experimental trials were attained only in duplicate.

**Table II: Differences in procedure pertaining to the Trials (n=6) of adsorption-desorption experiments.**

| Methods Section | Trial 1 | Trials 2-3 | Trials 4-6 |
|---|---|---|---|
| **2.1.2. Adsorbent Preparation** | • No preparation of GAC or NF was conducted. | • GAC was sieved and rinsed prior to adsorption.<br>• NF was not investigated. | • GAC was sieved and rinsed prior to adsorption.<br>NF was not investigated. |
| **2.1.4. Adsorption** | • Adsorption of GAC and NF occurred over a 7-day course at 5°C. | • Adsorption of GAC occurred over 24 hours at 5°C. | • Adsorption of GAC occurred over 24 hours at 5°C. |
| **2.1.5. Desorption** | • Desorption of GAC with sodium sulfide and occurred over a 7-day course at 22°C. | • Desorption of GAC with sodium sulfide occurred over 24 hours at 22°C.<br>• No decanting using replenishment of DI water prior to desorption was conducted. | • Desorption of GAC with sodium sulfide occurred over 24 hours at 22°C.<br>• Decanting of adsorbate was completed following adsorption, then replenished with DI water prior to desorption. |

### 2.1.2. Adsorbent Preparation

#### 2.1.2.1. GAC

Prior to introducing a sorbent material to the SRBR system, batch testing of adsorption and desorption mechanisms was conducted in triplicate. Approximately 3.8 g of 4-8 mesh GAC (Alfa Aesar, Stock 43118, Lot No. X18C004) was weighed, and then strained in a 2.0-mm No. 10 Newark sieve to remove fine particles as much as possible. The sieved GAC was weighed again and placed in a 300-mL Erlenmeyer flask, and filled with 300 mL of DI water. The GAC

was soaked in DI water for 24 hours to further remove fine particles. After 24 hours, the GAC was strained and rinsed in DI water, and then briefly air-dried.

#### 2.1.2.2. NF

For the preliminary trial using NF, approximately 7.5 g of NF was weighed and carefully placed inside a 300-mL Erlenmeyer flask. No adsorbent preparation was carried out for NF prior to adsorption.

### 2.1.3. Adsorbate Preparation

The adsorbate prepared for the batch adsorption experiments contained 5 mg/L $Cu^{2+}$ and 10 mg/L $Zn^{2+}$. Adsorbate was newly prepared in one-liter quantities to ensure consistency in concentration.

### 2.1.4. Adsorption

300 mL of adsorbate was placed in an Erlenmeyer flask along with the rinsed and dried GAC. The flasks were then sealed with Parafilm. The adsorbate and adsorbent remained at 5°C for 24 hours and occasionally swirled. After the adsorption duration was complete, a 25-mL sample was taken from the flask using a syringe in the absence of a filter for total recoverable analysis. An additional 25-mL sample was taken using a 0.45-µm filter (Fisherbrand MCE, Cat No. 09-720-005) applied to a syringe for dissolved metals analysis.

### 2.1.5. Desorption

After adsorption was complete, the flasks were decanted and replenished with 300 mL of DI water for Trials 4-6. Next, 50 mg of anhydrous sodium sulfide was added to each flask and then swirled for complete solute mixing. Trials 2-3 omitted decanting the adsorbate and replenishing with DI water prior to the addition of anhydrous sodium sulfide. The flasks were

sealed and maintained at 22°C for 24 hours of desorption and occasionally swirled. After 24 hours, 25-mL samples were collected for both total recoverable and dissolved metals analysis.

## 2.2. Sulfate-Reducing Bioreactor Experiments

### 2.2.1. Bioreactor Construction

The investigated bench-scale SRBR was a packed-bed upflow reactor contained in a 14-gallon polyethylene open-top drum (Figure 4). The system was initially constructed on 11/01/2016. Three holes were drilled into the drum for influent (bottom-right), effluent (top-left), and gas venting ports (very top). Connectors for tubing were placed inside the drilled holes and sealed using silicone caulking for anaerobic conditions and prevention of leaks. The influent flows in a bottom-up flow regime controlled by a peristaltic pump.

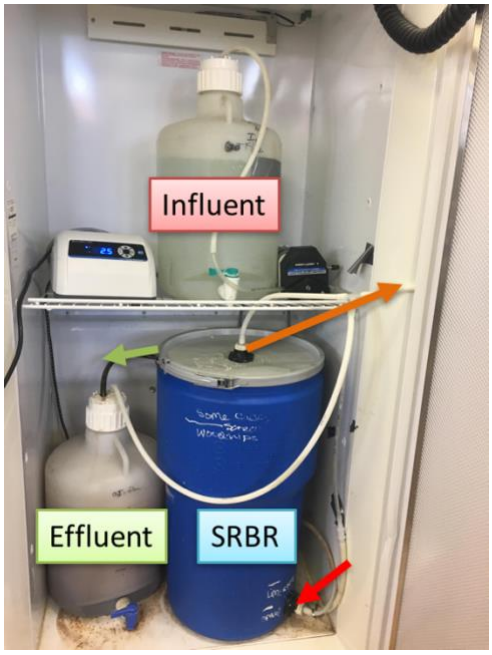


**Figure 4: Configuration of bench-scale sulfate-reducing bioreactor showing points of entry and exit of the influent (red), effluent (green), and gas vent (orange).**

The diameter of the reactor was 13 inches with 25 inches of depth reaching the effluent port. The depth occupied by substrate is 23 inches. Approximately 3.5 inches of gravel was

poured into the bottom of the reactor to allow for even distribution of flow, thereby preventing dead volume zones (Figure 5). Next, about one inch of limestone was added to buffer pH. Approximately 16.5 inches of woodchips were added next, with additional quantities of limestone mixed in. In total, there were three inches of limestone in the reactor. The woodchips were obtained from the Montana Tech Greenhouse. The woodchips were capped with an inch of limestone, not shown in Figure 5. An inch of gravel was placed on the top-most layer, with a fiberglass screen on top of the gravel to prevent woodchips from escaping. Three to four large rocks were placed on top of the screen to prevent floating or displacement of reactor components. Finally, the reactor was sealed and ready to incubate.

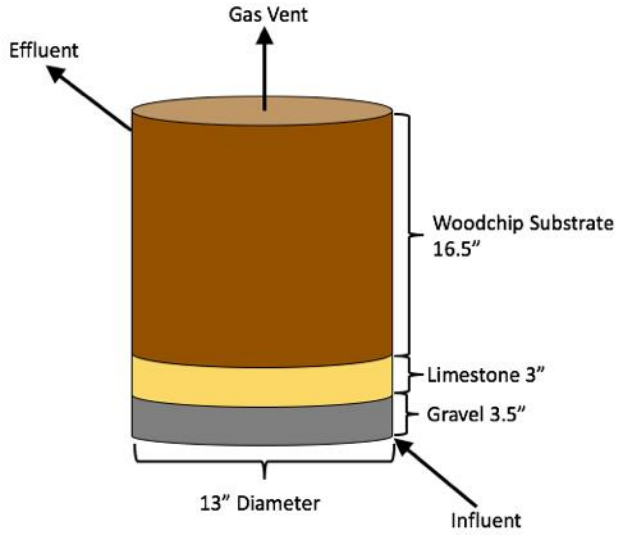


**Figure 5: Configuration of SRBRR with substrate components of woodchips, limestone and gravel represented as total quantities.**

### 2.2.2. Bioreactor Properties

The flow rate (Q) of the influent was 3.8 milliliters per minute (0.005472 $m^3$/day). The porosity, *e*, was determined to be 0.29 using a beaker test to measure the volume of voids with the woodchips used to construct the reactor. The total reactor volume, *V*, occupied by woodchip

substrate and void space was 0.035855 cubic meters. The theoretical hydraulic retention time, $\tau$, was 1.64 days (Eqn. 6)

$$\tau = \frac{eV}{Q} \tag{6}$$

#### 2.2.2.1. Growth of Sulfate-Reducing Bacteria

Once the reactor was constructed, the system was prepared for incubation. While incubating the system, a solution containing 1300 mg/L of $SO_4^{2-}$ was used to encourage growth of sulfate-reducing bacteria. Sulfate solution was continuously flowing into the reactor until satisfactory sulfate reduction was observed in the reactor effluent.

### 2.2.3. Experimental Design

#### 2.2.3.1. Influent Preparation

The influent consisted of prepared synthetic MIW containing 50 mg/L $Cu^{2+}$, 100 mg/L $Zn^{2+}$, and 1300 mg/L $SO_4^{2-}$ in solution. Solid anhydrous cupric sulfate, zinc sulfate monohydrate and anhydrous magnesium sulfate were carefully weighed using an analytical balance. The solutes were transferred to a one gallon container, in which one gallon of DI water was added, with thorough mixing to dissolve solutes. In total, five gallons of influent were prepared at a given time and replenished once consumed. In the event influent could not be immediately replenished, the peristaltic pump was paused and all potential sources of air from the tubing entering and exiting the reactor, except for the gas vent, were sealed using clamps. It was ensured that anaerobic conditions inside the reactor were maintained.

#### 2.2.3.2. Baseline Performance

The SRBR was initially operated under ambient air conditions in the laboratory at 22°C until 09/13/2017. The reactor effluent was sampled 2-5 times weekly from the effluent port. A large "stock" sample was collected during each sampling event. A 50-mL subsample was collected and immediately preserved with concentrated nitric acid for total recoverable metals analysis. Approximately 75 mL of effluent sample was filtered using a 0.45 µm membrane for dissolved elements and compounds analysis. Of this 75 mL, 50 mL was preserved with concentrated nitric acid for dissolved metals analysis. The remainder of the filtered effluent sample was immediately analyzed for dissolved sulfide and sulfate.

#### 2.2.3.3. Temperature Effects

Over the course of 1.5 months (09/13/2017 to 10/30/2017), the temperature of the incubator containing the SRBR was operated at 5°C. The reactor was operated and sampled in the same manner as described under baseline conditions. Samples were collected for total recoverable and dissolved metals, and dissolved sulfate and sulfide.

#### 2.2.3.4. Reactor Design Enhancements

##### 2.2.3.4.1. Addition of Granular Activated Carbon

Once adsorption/desorption experiments were complete, the reactor was opened on 10/24/2017 while microbial activity was minimal at a cold temperature. Large rocks used to prevent woodchips from escaping the reactor were removed temporarily. On top of the existing screen, 2 kg (~1-inch depth) of GAC was added as a new layer to the SRBR. There was adequate space inside the reactor for additional materials, as some substrate compaction and loss of limestone mass was expected to occur over time (USEPA, 2014). The GAC was levelled and an additional fiberglass screen was placed on top of the adsorbent (Figure 6). The selected quantity

of GAC was determined as an estimate based on batch adsorption experiments for one week of adsorption prior to breakthrough. The large rocks previously displaced were placed on top of the new top-most adsorbent layer. A small quantity of additional gravel (<1 inch) was added to prevent displacement of adsorbent and to optimize flow in the reactor (Figure 7). Immediately after the process of adding adsorbent to the reactor was complete, influent was fed into the system as previously carried out, and effluent was sampled the next day (10/25/2017).

**Figure 6: One-inch GAC layer added to the SRBR.**

**Figure 7: Gravel layer added on top of a fiberglass screen containing the GAC layer in the SRBR.**

#### 2.2.3.4.2. Adsorption

The reactor operated for an additional 7 days at 5°C with effluent samples collected every 2-4 days. Effluent parameters of total recoverable metals, total dissolved metals, sulfide, and sulfate were monitored every 2-5 days. Heavy metal analysis samples were preserved with nitric acid.

#### 2.2.3.4.3. Desorption

After 7 days of adsorption in the reactor at 5°C, the temperature was increased to 22°C for 28 days. Effluent samples were collected every 2-5 days. Heavy metal analysis samples were preserved with nitric acid. Analysis of effluent samples was conducted for total recoverable metals, total dissolved metals, dissolved sulfide, and dissolved sulfate.

## 2.3. Laboratory Analysis

Laboratory analyses were conducted to determine concentrations of dissolved sulfate and sulfide, and total recoverable and dissolved metals. Refer to Table III for USEPA or standard methods adopted by the manufacturer.

**Table III: Lab parameters, instrumentation, and EPA or standard methods.**

| Lab Parameter | Instrumentation | USEPA or Standard Method |
|---|---|---|
| Sulfate | HACH DR 6000 Spectrophotometer | HACH Method 10227 |
| Sulfide | HACH DR 6000 Spectrophotometer | EPA-Accepted HACH Method 8131 |
| Total Recoverable and Dissolved Metals | Thermo Scientific iCAP 6000 Series ICP-OES | EPA 200.7 |

### 2.3.1. HACH Spectrophotometer

Sulfate and sulfide concentrations were analyzed using a HACH DR 6000 Spectrophotometer.

#### 2.3.1.1. Sulfates

For detection of dissolved sulfates at a high range (150 – 900 mg/L $SO_4^{2-}$/L) the HACH TNT 865 turbidimetric method 10227 was employed. Sulfate samples were analyzed immediately after sample collection. Using the provided vials, 2 mL of filtered effluent or influent was pipetted into the vial. A levelled scoop (provided in each sulfate test kit) of barium chloride was added to the vial. A vial was inverted for one minute, and left to rest for 30 seconds before being placed in the spectrophotometer. The sample concentration was recorded in mg $SO_4^{2-}$/L. If the effluent sulfate concentration exceeded 900 mg/L, the test was repeated using a two-fold dilution.

#### 2.3.1.2. Sulfides

Excess sulfide was measured by analyzing for dissolved sulfides in the filtered effluent. The HACH Methylene Blue Method 8131 of low-range sulfide detection (5-800 µg $S^{2-}$/L) for spectrophotometers was employed. No allowable holding time exists for analysis of sulfide. Therefore, all sulfide samples were analyzed immediately after collection. Using a pipette, 10 mL of filtered effluent sample was transferred to a HACH square sample cell (Part no. 2495402). A blank was prepared by transferring 10 mL of DI water into an additional square cuvette. Next, 0.5 mL of Sulfide Reagent A was pipetted into the sample cell and swirled to mix. Once mixed, 0.5 mL of Sulfide Reagent B was pipetted into the sample cell and the cell was covered with Parafilm. The sample cell was thoroughly inverted for complete mixing. The sample cell was left undisturbed for five minutes prior to analysis. Once the five-minute time interval was complete, the blank cell was cleaned using a Kimwipe and placed into the HACH DR 6000 Spectrophotometer and the spectrophotometer was ‘zeroed’. The prepared samples were then placed in the spectrophotometer and the results were recorded in µg $S^{2-}$/L.

### 2.3.2. Inductively Coupled Plasma Optical Emissions Spectrometry

An inductively coupled plasma optical emissions spectrometer (ICP-OES; Thermo iCAP 6500 Duo 2008) was employed to determine the concentration of total recoverable and dissolved heavy metals in the reactor effluent and adsorption-desorption experiment samples. The ICP-OES was operated according to EPA Method 200.7 for analysis of heavy metals. The detection limit of the ICP-OES with respect to copper was 0.0025 mg/L and zinc was 0.0016 mg/L.

#### 2.3.2.1. Heavy Metal Sample Preparation

Due to the unavailability of a block digester, total recoverable and total heavy metals were digested according to EPA Method 200.7 using 400-mL beakers, trace metal grade nitric acid, 18 MΩ DI water, and hot plates. The temperature was monitored using a thermometer to ensure a constant temperature throughout the entirety of the acid digestion process.

## 2.4. Quality Assurance/Quality Control Measures

### 2.4.1. Sample Duplicates

Lab duplicates were sampled once per month from the reactor system (approximately once per 20 samples). Effluent duplicates samples were collected from the SRBR using the same methodology as per regular sample collection. All samples were analyzed in an identical manner. Adsorption and desorption experiments were all conducted in triplicate to demonstrate reproducibility of results.

### 2.4.2. Method Blanks

Method blanks were sampled once per month using DI water, and treated as regular samples for purposes of chemical analysis. Laboratory blanks were collected to determine the extent of contamination while conducting experiments. For purposes of ICP-OES analysis, calibration blanks were used during each run.

### 2.4.3. Calibration

High, medium, and low calibration standards were analyzed each time using the ICP-OES to ensure accurate results for the calibration curve. The validity of each calibration was confirmed using Initial Calibration Verification (ICV), Continuing Calibration Verification (CCV) and Continuing Calibration Blank (CCB) standards at first time ±5% accuracy and ±10% continued accuracy, according to EPA Method 200.7. Interference Check Solutions (ICSA and ICSAB) were employed to check for interferences. Sulfate standards were analyzed approximately once every two weeks in the HACH DR 6000 Spectrophotometer to ensure the instrument had maintained its accuracy. Automatic calibrations were performed by the HACH DR 6000 Spectrophotometer prior to each use.

## 2.5. Data Analysis

### 2.5.1. Batch Adsorption-Desorption Data

#### 2.5.1.1. Adsorption

Adsorption of heavy metals to the adsorbent was determined using mass balance calculations. Refer to Appendix A for example calculations pertaining to mass balances in select trials of batch adsorption and desorption experiments. All trials were completed in the same manner for the adsorption mass balance. Steady state conditions were assumed (Eqn. 7).

$$Metals\ Added = Metals\ Quantified \tag{7}$$

The source of metals into the mass balance was the initial dissolved concentrations of copper and zinc in in the adsorbate (Eqn. 8).

$$Metals\ Added = Initial\ Adsorbate\ Metals\ Input \tag{8}$$

The metals inputs equaled outputs, which consisted of metals adsorbed to GAC and PAC, and remaining metals in the dissolved phase that did not adsorb to activated carbon (Eqn. 9).

$$\begin{matrix}\textit{Metals} \\ \textit{Quantified}\end{matrix} = \begin{matrix}\textit{Metals} \\ \textit{Adsorbed} \\ \textit{to GAC}\end{matrix} + \begin{matrix}\textit{Metals} \\ \textit{Adsorbed} \\ \textit{to PAC}\end{matrix} + \begin{matrix}\textit{Dissolved} \\ \textit{Metals in} \\ \textit{Adsorbate}\end{matrix} \quad (9)$$

The difference between the initial adsorbate concentration and final adsorbate total dissolved metals concentration was the total metals adsorbed to the adsorbent (Eqn. 10).

$$\begin{matrix}\textit{Total Metals} \\ \textit{Adsorbed}\end{matrix} = \begin{matrix}\textit{Initial Metals} \\ \textit{Adsorbate Input}\end{matrix} - \begin{matrix}\textit{Total Dissolved Metals} \\ \textit{After Adsorption}\end{matrix} \quad (10)$$

The total adsorbed metals were the sum of metals adsorbed to GAC and PAC (Eqn. 11).

$$\begin{matrix}\textit{Total Metals} \\ \textit{Adsorbed}\end{matrix} = \begin{matrix}\textit{Metals Adsorbed} \\ \textit{to GAC}\end{matrix} + \begin{matrix}\textit{Metals Adsorbed} \\ \textit{to PAC}\end{matrix} \quad (11)$$

Metals adsorbed to PAC was determined by taking the difference between total recoverable metals and total dissolved metals after adsorption (Eqn. 12). Metals adsorbed to PAC were taken up by the syringe without a 0.45-µm filter.

$$\begin{matrix}\textit{Metals} \\ \textit{Adsorbed} \\ \textit{to PAC}\end{matrix} = \begin{matrix}\textit{Total Recoverable} \\ \textit{Metals after} \\ \textit{Adsorption}\end{matrix} - \begin{matrix}\textit{Total Dissolved} \\ \textit{Metals after} \\ \textit{Adsorption}\end{matrix} \quad (12)$$

Since total metals adsorbed and metals adsorbed to PAC were known after completing the above calculations, the final unknown, metals adsorbed to GAC, could be determined by taking the difference (Eqn. 13).

$$\begin{matrix}\textit{Metals} \\ \textit{Adsorbed} \\ \textit{to GAC}\end{matrix} = \begin{matrix}\textit{Total} \\ \textit{Metals} \\ \textit{Adsorbed}\end{matrix} - \begin{matrix}\textit{Metals} \\ \textit{Adsorbed} \\ \textit{to PAC}\end{matrix} \quad (13)$$

The fraction of metals removed by adsorption was calculated by taking the ratio of total metals adsorbed to the initial adsorbate metals input (Eqn. 14).

$$\textit{Fraction of Metals Adsorbed} = \frac{\textit{Total Metals Adsorbed}}{\textit{Initial Adsorbate Metals Input}} \quad (14)$$

#### 2.5.1.2. Desorption

The desorption of heavy metals from activated carbon had the potential to give rise to a variety of particle sizes. Prior studies have determined that copper sulfide and zinc sulfide particles existed in the nanometer range, depending on the method of synthesis (Dumbrava et al., 2005; Tank et al., 2017). Therefore, there was a possibility for metal sulfide particles to pass through a 0.45-µm filter, if the diameter of particles were less than 450 nm. Total recoverable metals analysis was utilized to account for the presence of nanoparticles.

##### 2.5.1.2.1. Trials 1-3

Desorption of heavy metals from GAC was assessed by comparing total recoverable metals concentrations before and after desorbing. The metals outputs in the mass balance following adsorption included total metals desorbed from GAC and PAC and metals remaining on GAC and PAC (Eqn. 15).

$$\begin{array}{lcllcllcl} \textit{Metals Out} & = & \textit{Total Metals Desorbed from GAC} & + & \textit{Total Metals Desorbed from PAC} & + & \textit{Metals Remaining on GAC} & + & \textit{Metals Remaining on PAC} \end{array} \quad (15)$$

The analysis of desorbed metals was focused on GAC. Total desorbed metals from GAC as precipitated metals were determined using the difference between total recoverable and total dissolved metal concentrations in the adsorbate after desorption (Eqn. 16).

$$\begin{array}{lcllcl} \textit{Total Precipitated Metals Desorbed from GAC} & = & \textit{Total Recoverable Metals after Desorption} & - & \textit{Total Recoverable Metals after Adsorption} \end{array} \quad (16)$$

The fraction of metals desorbed from GAC was calculated by taking the ratio of total metals desorbed to total metals adsorbed (Eqn. 17).

$$\textit{Fraction of Metals Desorbed from GAC} = \frac{\textit{Total Metals Desorbed from GAC}}{\textit{Total Metals Adsorbed to GAC}} \quad (17)$$

#### 2.5.1.2.2. Trials 4-6

Since decanting the adsorbate following desorption was a procedural difference in trials 4-6, the mass balance was altered accordingly. The metals out Eqn. (15) became (18), since the only sources of heavy metals in the flask follow desorption were metals desorbed from GAC and metals retained on GAC. Decanting of the adsorbate prior to desorption removed metals adsorbed to PAC and metals remaining in the dissolved phase.

$$\begin{array}{ccccc} \textit{Metals Out} & = & \textit{Total Metals Desorbed from GAC} & + & \textit{Metals Remaining on GAC} \end{array} \quad (18)$$

Eqn. (16) became (19), since the only source of heavy metals in adsorbate matrix was desorbed metals from GAC.

$$\begin{array}{ccccc} \textit{Total Metals Desorbed from GAC} & = & \textit{Precipitant Metals Desorbed from GAC} & = & \textit{Total Recoverable Metals after Desorption} \end{array} \quad (19)$$

Remaining desorption mass balance calculations remain the same as discussed in Methods section 2.5.1.2.1.

### 2.5.2. Sulfate-Reducing Bioreactor Data

#### 2.5.2.1. Sulfate Reduction

Sulfate reduction was monitored as the change in dissolved sulfate concentration ($\Delta S$, mg/L) from influent sulfate ($S_0$, mg/L) to effluent sulfate ($S$, mg/L) (Eqn. 20). It was assumed that any change in sulfate observed was accounted for by BSR. Sulfates lost from the influent were reduced to sulfide, and thereby utilized to precipitate heavy metals.

$$\Delta S = S - S_0 \quad (20)$$

#### 2.5.2.2. Heavy Metal Removal Efficiency

Filtered and total recoverable heavy metal concentrations were monitored in the effluent ($C_{out}$, mg/L) and represented as heavy metal removal efficiency (Eqn. 21). Influent heavy metal concentrations ($C_{in}$, mg/L) were held constant.

$$Efficiency = \frac{C_{in} - C_{out}}{C_{in}} \tag{21}$$

#### 2.5.2.3. Comparison to Sulfate Reduction Model

Experimental sulfate reduction data were compared to an ideal plug-flow reactor theoretical model to determine if the operated bioreactor performed as expected (Drury, 2000). A zero-order kinetics model was best suited to describe sulfate reduction (Eqn. 22) (Drury, 2017). The model predicted effluent sulfate ($S$) by the difference between influent sulfate ($S_0$) and a sulfate reduction term. The sulfate reduction term depended upon model inputs of organic matter conversion factors ($\eta$ = 0.78 and $f$ = 4 g $SO_4$/g carbon), ratio of solid volume to water volume of the substrate ($\beta$), degradation of organic matter ($G(t)$, g carbon/cm$^3$ and $k_G(t)$, year$^{-1}$), sulfate reduction rate coefficient ($k_s$, dimensionless) and hydraulic retention time ($\tau$). In this case, experimental effluent sulfate data were used to calculate the sulfate reduction rate coefficient and initial age that best fit the data using a sum of least squares analysis.

$$S = S_0 - \{f \beta \eta [k_G(t) G(t)] k_s \tau\} \tag{22}$$

The degradation rate of organic matter, $k_G(t)$, was calculated based on coefficients from the literature ($b$ = 0.16; $m$ = -1) and the reactor operating time, $t$ (Eqn. 23).

$$k_G(t) = b(a + t)^m \tag{23}$$

The ratio of solid volume to water volume of the substrate was calculated based on the substrate porosity ($e$ = 0.29) (Eqn. 24).

$$\beta = \frac{1 - e}{e} \tag{24}$$

Degradation of organic matter, *G(t)*, was inputted based on coefficients from the literature (*G(0)* = 0.084 g carbon/cm$^3$) and reactor operating time (Eqn. 25). Initial age, *a*, depended on the type of substrate and was required to be fit to the experimental data.

$$G(t) = G(0)\left(\frac{a + t}{a}\right)^{b} \tag{25}$$

# 3. Results & Discussion

## 3.1. Batch Adsorption-Desorption Trials

### 3.1.1. Granular Activated Carbon

#### 3.1.1.1. Trial 1

Trial 1 was conducted so that adsorption occurred for 7 days at 5°C and desorption occurred for 7 days at 22°C. The adsorbate solution contained approximately 5 mg/L copper and 10 mg/L zinc. In the first trial of adsorption over 7 days at 5°C, total recoverable copper was measured at 5.46 mg/L and total recoverable zinc was 9.25 mg/L (Table IV; Table V). Since the concentration of total recoverable copper was greater than 5 mg/L, it was assumed the initial input of copper was equal to 5.46 mg/L in Trial 1 only. At the same sampling time, total dissolved copper was 0.0578 mg/L and total dissolved zinc was 0.0256 mg/L (Table IV; Table V). In total, 5.41 mg/L (99%) of copper and 9.75 mg/L (98%) of zinc were adsorbed to both PAC and GAC (Table VI; Table VII). Of the 5.41 mg/L of copper that adsorbed to activated carbon, 5.41 mg/L adsorbed to PAC and 0 mg/L adsorbed to GAC (Table VI). Of the 9.75 mg/L of zinc, 9.00 mg/L adsorbed to PAC and 0.75 mg/L adsorbed to PAC (Table VII). Any further desorption to occur was solely attributed to PAC, since the amount of metals adsorbed to GAC was negligible.

After 7 days of desorption at 22°C, the total recoverable copper concentration was 4.48 mg/L and total recoverable zinc was 8.54 mg/L (Table IV; Table V). Mass balance calculations suggested that no copper or zinc desorbed from GAC (Table VI; Table VII). Since all nearly all of copper and zinc ions adsorbed to PAC, there was no possibility for heavy metals to desorb from GAC (Table VI; Table VII). The potential for desorption was assessed by attaining non-zero desorption yields from GAC. Therefore, meaningful conclusions for desorption were not drawn from Trial 1 due to interference of PAC adsorption.

#### 3.1.1.2. Trials 2-3

Trials 2-3 were modified so that adsorption occurred over 24 hours at 5°C and desorption occurred for 24 hours at 22°C.

##### 3.1.1.2.1. Qualitative Testing

Trials 2 and 3 after 24 hours of adsorption were shown as the first two flasks in Figure 8. The third flask depicted in Figure 8 was compromised and could not be analyzed. Following 24 hours after the addition of sodium sulfide, there was evidence of interaction between the metals, suggesting precipitation of metal sulfides (Figure 9). The color of the adsorbate solution changed from clear to green (Figure 9). Two samples were drawn using a syringe from one of the flasks depicted in Figure 9. One unfiltered sample was transferred to a test-tube, while the second sample was filtered using a 0.45-μm filter and transferred to a second test-tube (Figure 10). The test tube on the left showed the unfiltered sample, with green adsorbate solution (Figure 10). The test tube on the right showed the clear filtered sample (Figure 10). Qualitatively, this reinforced the mechanism of precipitation of heavy metal sulfides after adding sodium sulfide to a flask with adsorbed copper and zinc. A blank was qualitatively tested by adding DI water to activated carbon for 24 hours. Once 24 hours passed, sodium sulfide was added to the flask and the color of the adsorbate remained clear. After an additional 24 hours, the flask remained clear with no apparent changes.

**Figure 8: Twenty-four hours after addition of copper and zinc MIW solution to GAC at 5°C.**

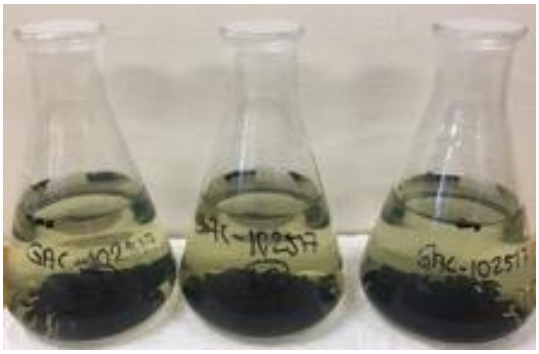

**Figure 9: Twenty-four hours after addition of sodium sulfide to GAC at 22°C with resultant desorbed copper and zinc sulfides.**

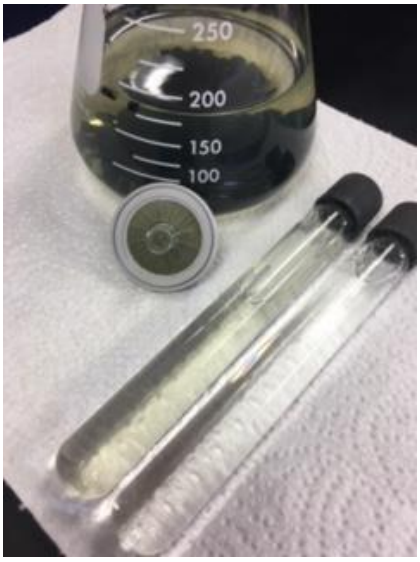


**Figure 10: Twenty-four hours after addition of sodium sulfide to GAC at 22°C with resultant desorbed copper and zinc sulfides. Total recoverable sample (left) and filtered sample (right).**

#### 3.1.1.2.2. Trial 2

After adsorption occurred throughout Trial 2, total recoverable copper was 1.81 mg/L and total recoverable zinc was 4.09 mg/L (Table IV; Table V). Total dissolved samples after adsorption indicated 0.201 mg/L of copper and 0.446 mg/L of zinc were remaining in the adsorbate (Table IV; Table V). Total copper adsorption to activated carbon was 4.80 mg/L (96%) (Table VI). Of the 4.80 mg/L of copper that adsorbed, 1.61 mg/L adsorbed to PAC and 3.19 mg/L adsorbed to GAC (Table VI). Total zinc adsorption to activated carbon was 9.55 mg/L (96%), of which 3.64 mg/L of zinc adsorbed to PAC and 5.91 mg/L adsorbed to GAC (Table VII). Trial 2 results showed efforts to wash away PAC were somewhat effective, but not completely. Total recoverable metals sample concentrations initially after adsorption indicated PAC could not be removed entirely.

After desorption during Trial 2, the concentration of total recoverable copper was 4.70 mg/L and zinc was 7.31 mg/L (Table IV; Table V). Attributed to GAC, total copper desorption was 2.90 mg/L (91%) and total zinc desorption was 3.22 mg/L (55%) (Table VI; Table VII). In Trial 2, a greater quantity of heavy metals adsorbed to GAC than PAC, which allowed for desorption and precipitation of heavy metals from GAC.

Trial 2 suggested positive results in favor of desorption of copper and zinc precipitants, with potential for further use of the regenerated GAC. Selectivity in favor of copper desorption was occurring in mixed copper and zinc adsorbate.

#### 3.1.1.2.3. Trial 3

After the adsorption period during Trial 3, total recoverable copper was 3.51 mg/L and total dissolved copper was 0.339 mg/L (Table IV). Total recoverable zinc was 6.93 mg/L and total dissolved zinc was 2.37 mg/L (Table V). Resultant copper adsorption was 4.66 mg/L

(93%), with 3.17 mg/L adsorbed to PAC and 1.49 mg/L adsorbed to GAC (Table VI). Zinc adsorption was 7.63 mg/L with 4.56 mg/L adsorbed to PAC and 3.07 mg/L adsorbed to GAC (Table VII).

After desorption, total recoverable copper was 3.85 mg/L and total dissolved copper was 0.427 mg/L (Table IV). Total recoverable zinc was 7.37 mg/L and total dissolved zinc was 0.519 mg/L (Table V). In total, 0.342 mg/L (23%) of copper and 0.442 mg/L (14%) of zinc desorbed from GAC. A greater quantity of heavy metals initially adsorbed to PAC than GAC, therefore, there was a limited potential for desorption from GAC. Trial 3 supported the potential of heavy metal desorption from GAC, despite lower yields of desorption.

#### 3.1.1.3. Trials 4-6

Trials 4-6 were done in triplicate, following the final procedural modifications described in Methods sections 2.1.2 to 2.1.5. GAC was sieved, soaked and rinsed over 24 hours prior to adsorption. Adsorption occurred over 24 hours at 5°C. Following adsorption, the adsorbate was decanted and replenished with an equivalent volume of DI water prior to desorption to further alleviate PAC interference. Desorption occurred over 24 hours at 22°C. Through the process of decanting after adsorption, it was assumed only GAC contributed to desorption. Therefore, PAC was removed from the mass balance for Trials 4-6.

##### 3.1.1.3.1. Trial 4

After adsorption in Trial 4, total recoverable copper was 2.56 mg/L and total dissolved copper was 0.732 mg/L (Table IV). Total recoverable zinc was 5.46 mg/L and total dissolved zinc was 3.91 mg/L (Table V). In total, 4.27 mg/L (84%) of copper adsorbed to GAC, with 1.83 mg/L adsorbed to PAC and 2.44 mg/L adsorbed to GAC (Table VI). Total zinc adsorption was

6.09 mg/L (61%), consisting of 1.55 mg/L adsorbed to PAC and 4.54 mg/L adsorbed to GAC (Table VII).

Following desorption, the total recoverable copper concentration was 4.33 mg/L and total dissolved copper was 0.688 mg/L (Table IV). Total recoverable zinc was 8.00 mg/L and total dissolved zinc was 2.31 mg/L (Table V). Attributed to GAC, copper desorption was 4.33 mg/L (178%) and total zinc desorption was 8.00 mg/L (176%) (Table VI; Table VII). Trial 4 did not provide meaningful results and was considered an outlier, since the mass balance revealed >100% desorption.

#### 3.1.1.3.2. Trial 5

Trial 5 did not show success in desorbing GAC. During Trial 5, 4.15 mg/L (83%) of copper adsorbed to activated carbon, with 1.73 mg/L adsorbed to PAC and 2.41 mg/L adsorbed to GAC (Table VI). With respect to zinc, 1.75 mg/L adsorbed to PAC and 3.79 mg/L adsorbed to GAC, and in total 5.53 mg/L (55%) (Table VII). Total desorption of copper from GAC was 0.458 mg/L (19%), and zinc was 0.674 mg/L (18%) (Table VI; Table VII). Although limited, Trial 5 supported the potential for desorption of heavy metals from GAC.

#### 3.1.1.3.3. Trial 6

Trial 6 showed similar results to Trial 5. Throughout Trial 6, 4.12 mg/L (82%) of copper adsorbed to activated carbon, with 1.99 mg/L adsorbed to PAC and 2.13 mg/L adsorbed to GAC (Table VI). Zinc adsorbed entirely to PAC with a total of 6.68 mg/L (68%) (Table VII). Total copper desorption from GAC was 0.495 mg/L (23%) (Table VI). No desorption of zinc from GAC was achieved, as the entirety of zinc in the adsorbate adsorbed to PAC (Table VII). Trial 6 supported the potential for copper desorption from GAC.

**Table IV: Copper concentrations following Trials (n=6) of GAC adsorption and desorption using mixed copper and zinc solution.**

| Sample | | Trial 1 | 2 | 3 | 4 | 5 | 6 |
|---|---|---|---|---|---|---|---|
| Adsorption | Total Recoverable Copper (mg/L) | 5.46 | 1.81 | 3.51 | 2.56 | 2.59 | 2.87 |
| | Total Dissolved Copper (mg/L) | 0.0578 | 0.201 | 0.339 | 0.732 | 0.854 | 0.880 |
| Desorption | Total Recoverable Copper (mg/L) | 4.48 | 4.70 | 3.85 | 4.33 | 0.458 | 0.495 |
| | Total Dissolved Copper (mg/L) | 0.0256 | 1.04 | 0.427 | 0.688 | 0.140 | 0.306 |

**Table V: Zinc concentrations following Trials (n=6) of GAC adsorption and desorption using mixed copper and zinc solution.**

| Sample | | Trial 1 | 2 | 3 | 4 | 5 | 6 |
|---|---|---|---|---|---|---|---|
| Adsorption | Total Recoverable Zinc (mg/L) | 9.25 | 4.09 | 6.93 | 5.46 | 6.21 | 10.8 |
| | Total Dissolved Zinc (mg/L) | 0.250 | 0.446 | 2.37 | 3.91 | 4.47 | 4.09 |
| Desorption | Total Recoverable Zinc (mg/L) | 8.54 | 7.31 | 7.37 | 8.00 | 0.674 | 0.842 |
| | Total Dissolved Zinc (mg/L) | 0.125 | 0.840 | 0.519 | 2.31 | 0.321 | 0.563 |

**Table VI: Trials (n=6) of GAC regeneration data of copper beginning with addition of mixed dissolved copper (5 mg/L) and zinc (10 mg/L) solution, followed by sodium sulfide.**

| | Adsorbed Copper (mg/L) | | | Total Copper Desorbed from GAC (mg/L) |
|---|---|---|---|---|
| Trial | PAC | GAC | Total | |
| 1 | 5.41 | 0.00 | 5.41 (99%) | 0.00 (0%) |
| 2 | 1.61 | 3.19 | 4.80 (96%) | 2.90 (91%) |
| 3 | 3.17 | 1.49 | 4.66 (93%) | 0.342 (23%) |
| 4 | 1.83 | 2.44 | 4.27 (84%) | - |
| 5 | 1.73 | 2.41 | 4.15 (83%) | 0.458 (19%) |
| 6 | 1.99 | 2.13 | 4.12 (82%) | 0.495 (23%) |

**Table VII: Trials (n=6) of GAC regeneration data of zinc beginning with addition of mixed dissolved copper (5 mg/L) and zinc (10 mg/L) solution, followed by sodium sulfide.**

| | Adsorbed Zinc (mg/L) | | | Total Zinc Desorbed from GAC (mg/L) |
|---|---|---|---|---|
| Trial | PAC | GAC | Total | |
| 1 | 9.00 | 0.754 | 9.75 (98%) | 0.00 (0%) |
| 2 | 3.64 | 5.91 | 9.55 (96%) | 3.22 (55%) |
| 3 | 4.56 | 3.07 | 7.63 (76%) | 0.442 (14%) |
| 4 | 1.55 | 4.54 | 6.09 (61%) | - |
| 5 | 1.75 | 3.79 | 5.53 (55%) | 0.674 (18%) |
| 6 | 6.68 | 0 | 6.68 (67%) | 0.00 (0%) |

#### 3.1.1.4. Interpretation of Batch GAC Adsorption and Desorption Experiments

Overall, the results of the batch adsorption-desorption experiments were highly variable. Variability in results were best explained by interactions with PAC. Since physical adsorption was a nonspecific binding mechanism, it was possible sulfide ions interacted with the surface of the activated carbon, and did not fully contact the adsorbed metals in trials with lower yields of desorption. The trials that presented potential for desorption attributed to GAC indicated evidence that regeneration occurred. Previous research indicated desorption of copper in a column of GAC using a basic sodium hydroxide solution was achieved in under 30 minutes (Mugisidi et al., 2007). Therefore, there was relevance in employing a basic anion, sulfide, to desorb and precipitate heavy metals for regeneration of GAC.

The mixed heavy metals adsorbed by GAC was approximately 1.18 mg/g (Appendix B). To accurately determine the adsorption capacity, adsorption isotherms should be created. This ratio of adsorbed divalent metals to adsorbent mass was used to determine the theoretical breakthrough time of adsorbed heavy metals in the SRBR with the addition of adsorbent.

### 3.1.2. Natural Fibers

The potential of NF to adsorb heavy metals during cold temperature conditions and to desorb metal sulfides during ambient conditions was evaluated. After adsorption, total recoverable copper was 0.912 mg/L and total dissolved copper was 0.924 mg/L (Table VIII). Total recoverable zinc was 3.47 mg/L and total dissolved zinc 3.17 mg/L (Table VIII). In total, 4.08 mg/L (82%) of copper and 6.83 mg/L (68%) of zinc adsorbed to NF (Table IX). No evidence of desorption occurred, as there was no increase in the total recoverable heavy metal concentrations of copper and zinc following desorption (Table VIII; Table IX).

**Table VIII: Copper and zinc concentrations following one trial of NF adsorption and desorption using mixed copper and zinc adsorbate.**

| Sample | | Copper | Zinc |
|---|---|---|---|
| **Adsorption** | **Total Recoverable Metals (mg/L)** | 0.912 | 3.47 |
| | **Total Dissolved Metals (mg/L)** | 0.924 | 3.17 |
| **Desorption** | **Total Recoverable Metals (mg/L)** | 0.875 | 2.37 |
| | **Total Dissolved Metals (mg/L)** | 1.16 | 2.33 |

**Table IX: One trial of NF regeneration data of zinc beginning with addition of mixed dissolved copper and zinc adsorbate, followed by sodium sulfide.**

| Metal | Total Adsorbed Metals (mg/L) | Total Desorbed Metals (mg/L) |
|---|---|---|
| **Cu** | 4.08 (82%) | 0.00 (0%) |
| **Zn** | 6.83 (68%) | 0.00 (0%) |

### 3.1.3. Selection of Adsorbent

The purpose of Trial 1 of the GAC and NF batch regeneration experiments was to select the optimum adsorbent material for use within the SRBR. Based on Trial 1, GAC was selected to improve cold temperature performance of the SRBR. The mass required for NF to adsorb 300 mL of MIW (5 mg/L copper and 10 mg/L zinc) was nearly twice of GAC required. Greater removal of heavy metals was achieved using 3.8 g of GAC than 7.5 g of NF. As well, NF occupied nearly the entire volume of the Erlenmeyer flask, whereas a minimal volume of GAC occupied the flask to achieve the same amount of adsorption. The density and specific surface area of GAC is greater than NF, meaning GAC will adsorb more heavy metals and occupy less volume at a larger scale to achieve the same result. While a reactor should be scaled up as required, minimizing the footprint of a full-scale SRBR as much as reasonably possible is ideal. Based on the composition of NF, it is likely that the fibers themselves will degrade in the reactor and be used as an electron donor for BSR (Tripetchkul et al., 2012). The physical and chemical

composition of GAC is more stable, and would likely persist in the SRBR for a greater duration of time.

For long-term applications, GAC was determined to be a more feasible choice, despite faster adsorption kinetics among PAC and nearly trace quantities required in some instances. Implementation of PAC would not be practicable for stream remediation to supplement SRBR performance in winter months. The use of PAC in water treatment is practical when applied as a pre-treatment process prior to membrane filtration, or when easily recovered (Crittenden et al., 2012). Maintaining hydraulic conductivity in an SRBR would not be achieved with the use of PAC.

## 3.2. Sulfate-Reducing Bioreactor Operation

### 3.2.1. Sulfate Reduction

#### 3.2.1.1. Experimental Sulfate Reduction Data

##### 3.2.1.1.1. Baseline Performance

Sulfate reduction was at its peak during baseline operation (at 22°C) from 04/05/2017 to 09/11/2017 (Figure 11). While at baseline, average sulfate reduction was 370 mg $SO_4^{2-}$/L, ranging from 282 to 498 mg/L. Baseline reactor performance was adequate for the required sulfate reduction to precipitate and immobilize the influent metals dissolved concentrations of 100 mg/L Zn and 50 mg/L Cu. The minimum sulfate reduction based on influent heavy metal loadings was 223 mg/L, based on stoichiometry (Appendix B). The mean sulfate reduction was converted to an approximate removal rate of 588 mmol/$m^3$/d, based on reactor volume and influent flow rate. Experiments conducted by Eger (1992) found average sulfate removal rates of 125-490 mmol/$m^3$/d, averaging at approximately 300 mmol/$m^3$/d. Evidently, the reactor size and influent flow rate were appropriately scaled for baseline conditions to sufficiently treat influent heavy metals.

#### 3.2.1.1.2. Cold Temperature Performance

Altering the incubator temperature to 5°C (09/12/2017 to 10/24/2017) resulted in lower sulfate reduction, averaging 151 mg/L and ranging from 54 to 467 mg/L (Figure 11). At this temperature, the average sulfate reduction was not adequate for 98% heavy metal precipitation (223 mg/L required). The average sulfate reduction at 5°C was converted into an average sulfate removal rate of 239 mmol/$m^3$/d, which was lower than the desired rate of 300 mmol/$m^3$/d (Eger, 1992). This was representative of subsequent effluent heavy metal concentrations in the absence of a secondary mechanism of adsorption (Figure 16). Inhibited sulfate reduction was observed 09/16/2017 – four days following the temperature drop. Therefore, BSR activity was not instantaneously impacted by the temperature drop.

Results reinforced the requirement for a design improvement to SRBR systems operating under cold temperature conditions. The resultant sulfate reduction from one month of operation at 5°C was inadequate to produce desired heavy metal removal efficiency (>98% removal).

#### 3.2.1.1.3. Addition of Adsorbent

The addition of GAC to the bioreactor showed that adsorption influenced effluent sulfate concentration. From 10/25/2017 to 11/06/2017, effluent sulfate reduction increased to a maximum of 489 mg/L. This observed increase in sulfate removal was not attributed to microbial activity. Prior studies showed activated carbon (22-38% sulfate removal) and coconut coir pith adsorb sulfate in solution at comparable concentrations and neutral pH conditions (Salmon, 2009; Namasivayam, 2008). Consequently, sulfate adsorption must be considered in full-scale design.

During final two days of operation at 5°C after adding GAC to the system, freezing of the bottom five inches of the bioreactor was observed. Abnormally low effluent flow and frost

forming along the walls of the incubator prompted the investigation of internal freezing in the bioreactor. Using an infrared temperature sensor, freezing was observed within the reactor. The sensor detected temperatures below 0°C when oriented towards the bottom five inches of depth of the bioreactor. At depths above five inches, the sensor detected temperatures above 0°C.

Effluent sulfate was further monitored after the incubator temperature was resumed to 22°C on 11/06/2017. It was observed that sulfate reduction did not recover as quickly as anticipated. After GAC breakthrough occurred, sulfate reduction dropped to 133 mg/L, and ranged from 96 to 160 mg/L 11/06/2017 to 12/05/2017. Sulfate reduction notably increased 1/10/2018 to 1/24/2018 – varying from 176 to 203 mg/L.

However, sulfate reduction did not increase to baseline conditions as rapidly as predicted (Figure 11). Prior research indicated winter freezing had little effect on an SRBR with a well-established bacterial population (Neculita et al., 2007). Sulfate-reducing bacteria have been documented to have survived under harsh climates (Postgate, 1984). However, the rate of organic matter decay declines with temperature (Gusek, 2004). This process is likely more time consuming than resuming baseline conditions with no occurrence of freezing.

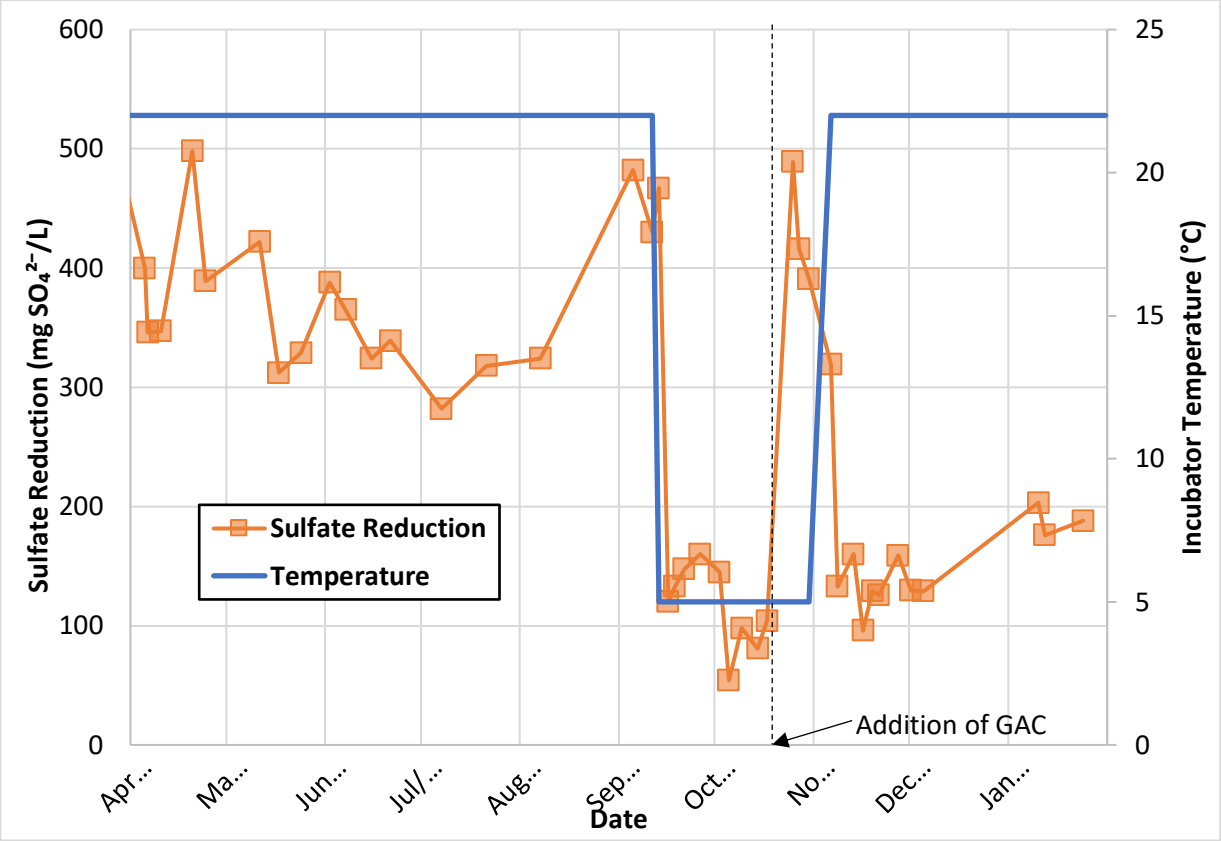


**Figure 11: SRBR sulfate reduction represented as the difference from influent to effluent sulfate concentration (mg $SO_4^{2-}$/L) 04/05/2017 to 01/24/2018.**

#### 3.2.1.2. Sulfate Reduction Model

Sulfate reduction operating at 22°C from 3/29/2017 to 9/13/2017 was best described by an initial age of 0.5 years (Figure 12). Fitting experimental data to the model, the resultant zero-order sulfate reduction rate coefficient of baseline SRBR operation was 0.581.

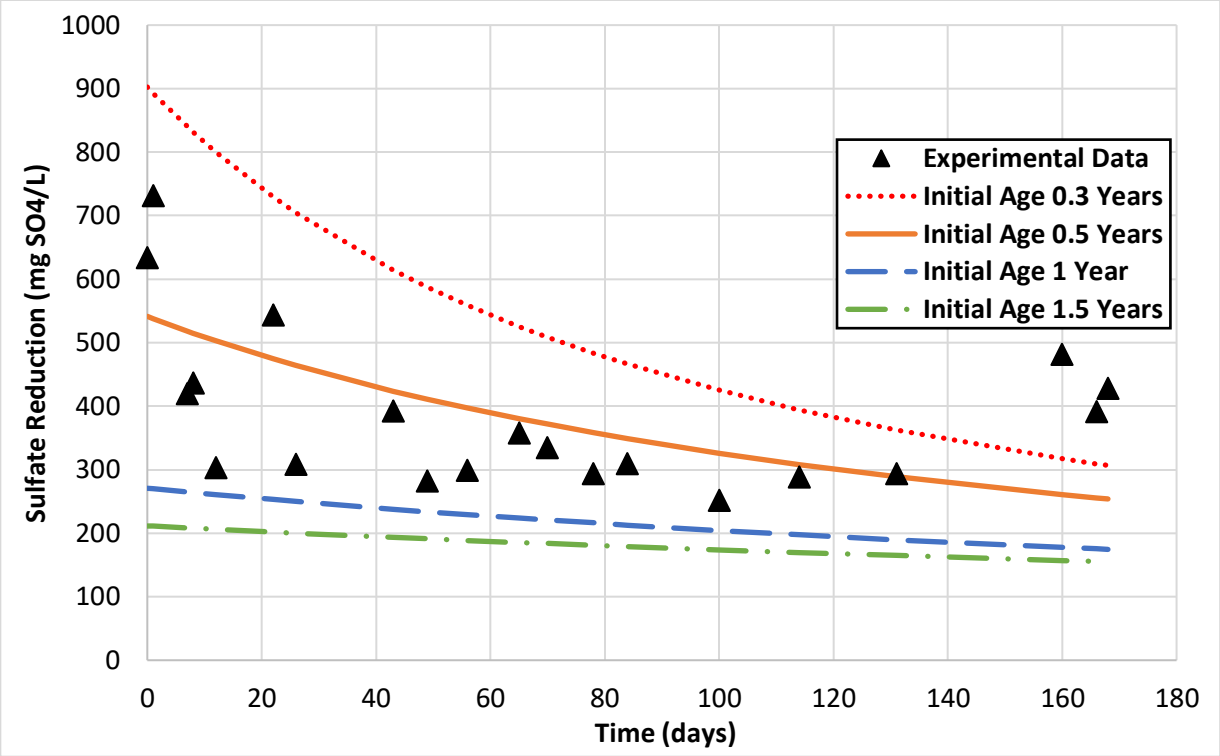


**Figure 12: Modelled sulfate reduction (mg/L) against experimental data 0 to 168 days of SRBR operation at 22°C prior to GAC addition (3/29/2017 to 9/13/2017).**

Operating the SRBR at 5°C (9/16/2017 to 10/17/2017) prior to GAC addition, the experimental data best fit the sulfate reduction model at an initial age of 0.5 years (Figure 13). The resultant zero-order sulfate reduction rate coefficient operating at 5°C was 0.295. By significantly decreasing the incubator temperature, the sulfate reduction rate coefficient declined by nearly one half.

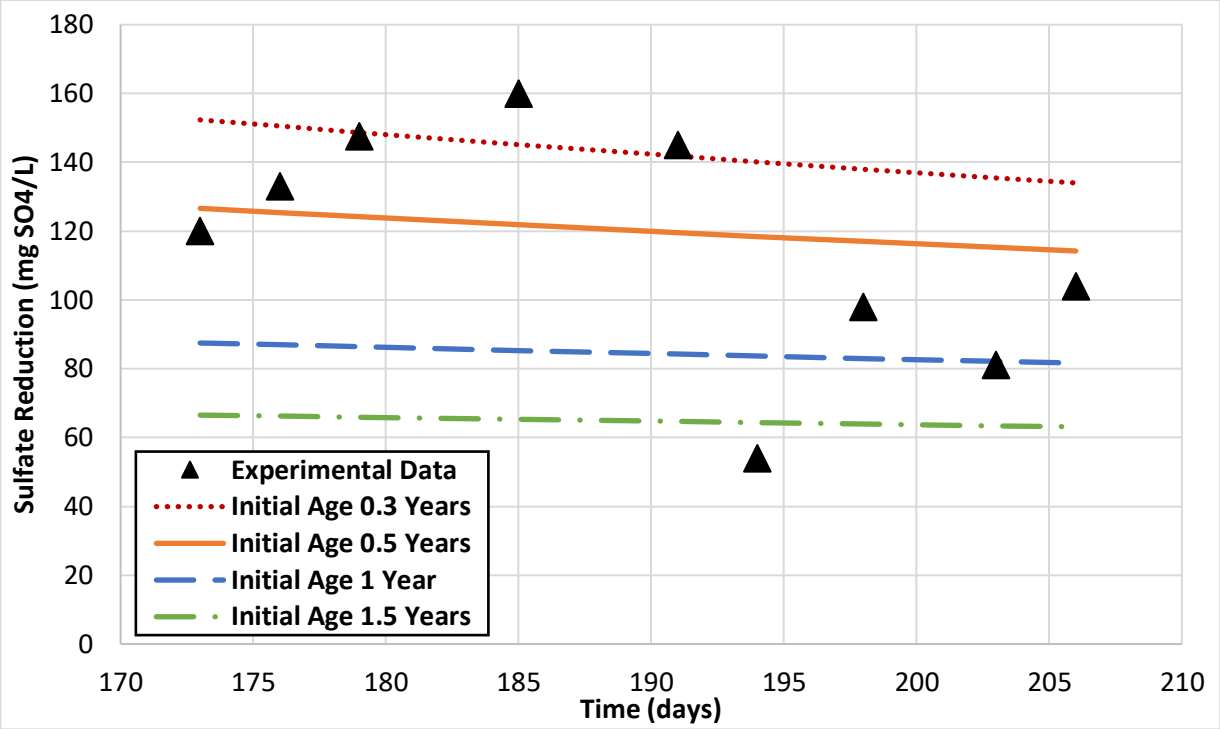


**Figure 13: Modelled sulfate reduction (mg/L) against experimental data 173 to 206 days of SRBR operation at 5°C prior to GAC addition (9/16/2017 to 10/17/2017).**

### 3.2.2. Excess Sulfides

Excess sulfides coincided with sulfate removal up until the addition of GAC to the SRBR system (Figure 14). The highest effluent excess concentrations were observed 09/21/2017 to 09/26/2017, ranging from 14 to 18 µg/L and averaging 16 µg/L. Despite the fact these results attained during 5°C operation, during this period, sulfate reduction was not yet at its minimum (Figure 11). A significant drop in excess sulfide concentrations was observed during 5°C operation 10/02/2017 to 10/20/2017. During this stage, excess sulfides ranged from 7 to 9 µg/L, averaging at 8 µg/L. After GAC addition and operating at 5°C, there was no significant change in excess sulfide (average 7 µg/L).

After increasing the temperature to 22°C, sulfide ranged from 5-7 µg/L and averaging at 6.5 µg/L (Figure 14). On 1/24/2018, a value of excess sulfide below the minimum detection level

was observed at 3 µg/L. The significance of a value below detection pertained to the objectives of this study, and was included in the interpretation of results. During this period, excess sulfide was not proportional to sulfate reduction rate (Figure 11). Sulfate reduction during January 2018 was 176-203 mg/L, pairing with excess sulfide values of 6 µg/L. While operating at 5°C, from 9/21/2017 to 9/26/2017, change in sulfate measurements of 145-160 mg/L paired with excess sulfide levels of 15-18 µg/L.

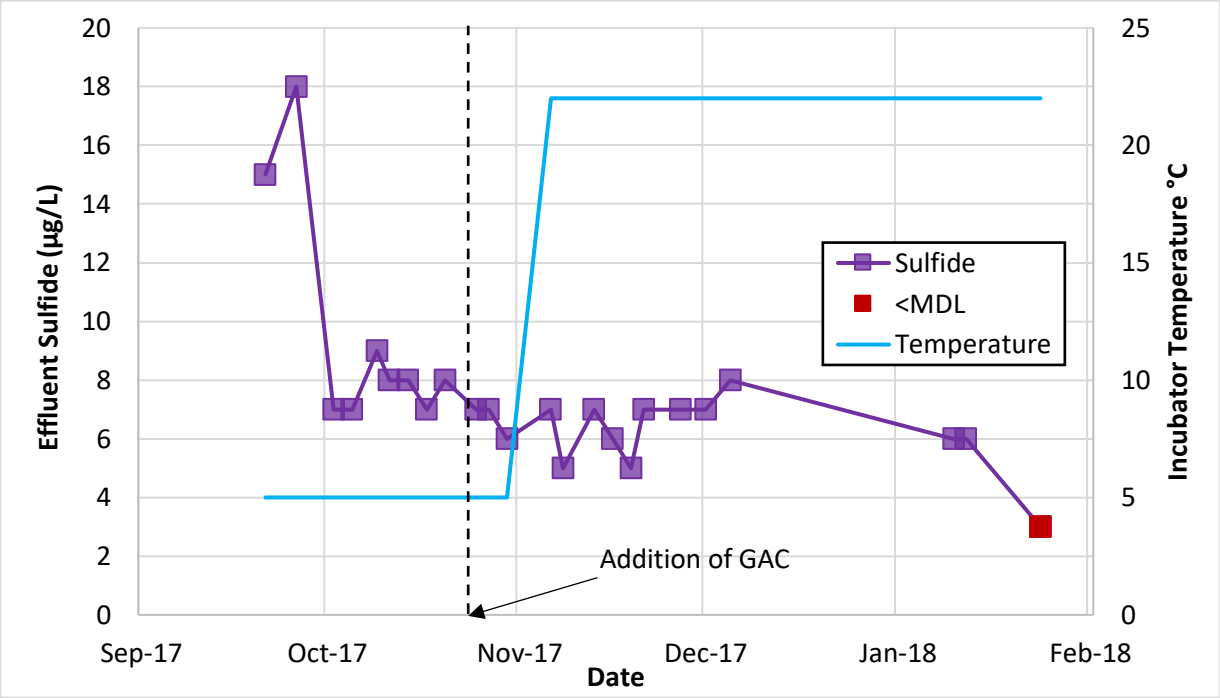


**Figure 14: SRBR effluent dissolved sulfide concentration (µg $S^{2-}$/L) 09/21/2017 to 01/24/2018 with <MDL in red.**

It was interpreted that excess sulfide absent in the effluent was utilized elsewhere in the SRBR. Particularly, the excess sulfide may be consumed by desorption and precipitation of sequestered metals in the GAC added to the SRBR. In the event desorption was not occurring, correspondingly greater concentrations of excess sulfides would be expected. Once regeneration of GAC is theoretically complete, excess sulfides may resume to greater concentrations in the

SRBR effluent. Prior results supported this predicted mechanism. Specifically, total recoverable copper was significantly greater than paired total dissolved measurements.

### 3.2.3. Heavy Metal Removal Efficiency

#### 3.2.3.1. Baseline Performance

During baseline reactor operation at 22°C, removal of dissolved copper was 99.6% to 99.96% (average 99.8%, 0.11 mg/L), and total recoverable copper was 99.7% to 99.8% (average 99.8%, 0.13 mg/L) (Figure 15; Figure 16). The removal efficiency of dissolved zinc ranged from 98.3% to 99.9%, averaging at 99.1% (0.91 mg/L). Total recoverable zinc removal was 97.8% to 99.0%, averaging at 98.4% (1.64 mg/L).

#### 3.2.3.2. Cold Temperature Performance

Once the incubator temperature was adjusted to 5°C on 09/13/2017, dissolved copper removal ranged from 92.9% to 99.98% (average 96.9%, 1.56 mg/L), and total recoverable copper varied between 88.5% to 99.8% (average 94.0%, 3.01 mg/L) (Figure 15; Figure 16). Dissolved zinc was 52.5% to 99.91% (average 75.9%, 24.1 mg/L), and total recoverable zinc was 52.0% to 99.0% (average 74.4%, 25.6 mg/L). During cold temperature operation, peak values of heavy metal removal efficiency were observed 12 hours after the incubator temperature dropped. Minimum removal efficiencies occurred after one month of operation under cold temperature conditions.

#### 3.2.3.3. Addition of Adsorbent

GAC was added to the bioreactor on 10/24/2017. After the addition of GAC to the SRBR operating at 5°C 10/25/2017 to 11/06/2017, a considerable increase in heavy metal removal efficiency was observed during this time frame (Figure 15; Figure 16). Heavy metal removal efficiency of total dissolved copper was 99.1% to 99.4%, averaging at 99.2% (0.38 mg/L). Total

recoverable copper removal ranged from 91.2% to 98.3% at an average of 95.9% (2.04 mg/L). Total dissolved zinc removal was 93.0% to 96.9% with an average of 95.4% (4.60 mg/L). Removal of total recoverable zinc ranged from 84.7% to 94.3%, averaging at 90.2% (9.78 mg/L).

Effluent heavy metal removal efficiency was monitored after returning the SRBR to 22°C on 11/06/2017 after the adsorption period in the SRBR at 5°C. Copper removal rapidly recovered to baseline conditions (>98% removal) (Figure 15; Figure 16). The response in the recovery of zinc removal was delayed, recovering to 75.6% removal over a period of two months. Total dissolved copper removal varied from 97.7% to 99.9% (average 99.4%, 0.28 mg/L). The removal efficiency of total recoverable copper was 96.6% to 99.94%, averaging at 98.6% (0.69 mg/L). Total dissolved zinc removal was 52.4% to 96.8%, averaging at 70.8% (29.2 mg/L). Removal of total recoverable zinc was 49.2% to 95.8% (average 69.3%, 30.7 mg/L).

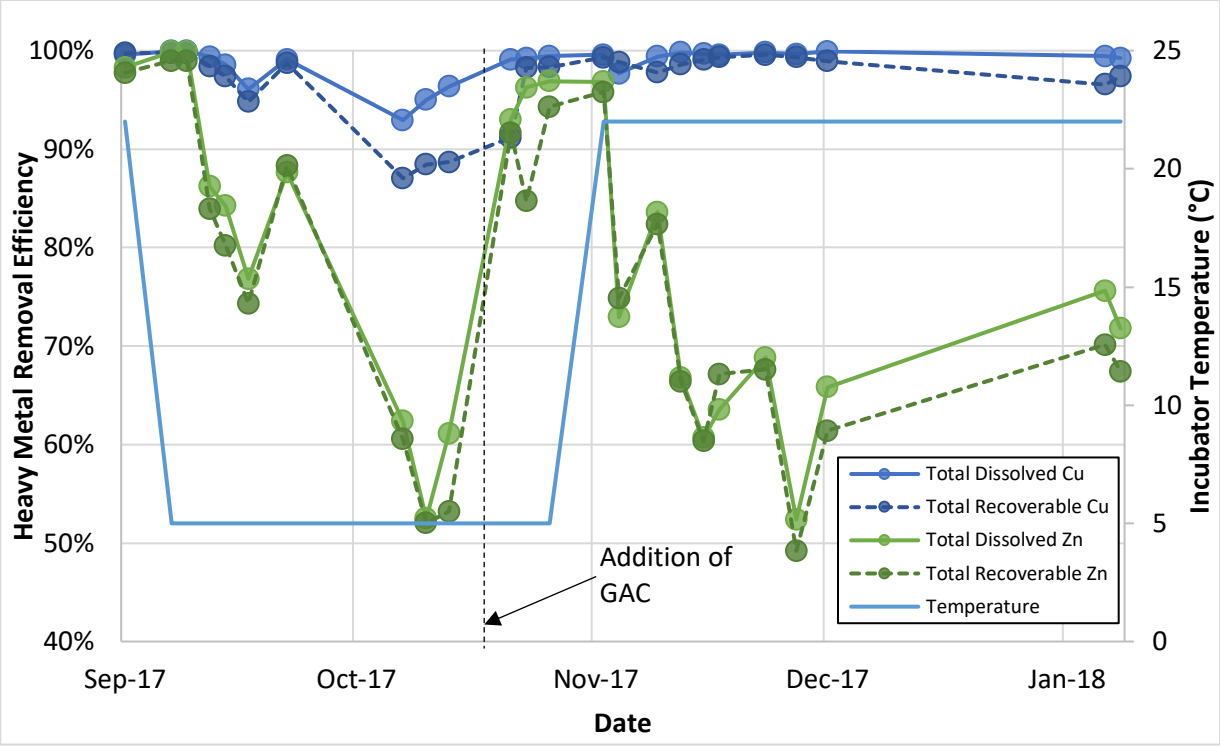


**Figure 15: SRBR heavy metal removal efficiency of total recoverable and dissolved copper and zinc 09/02/2017 to 01/12/2018.**

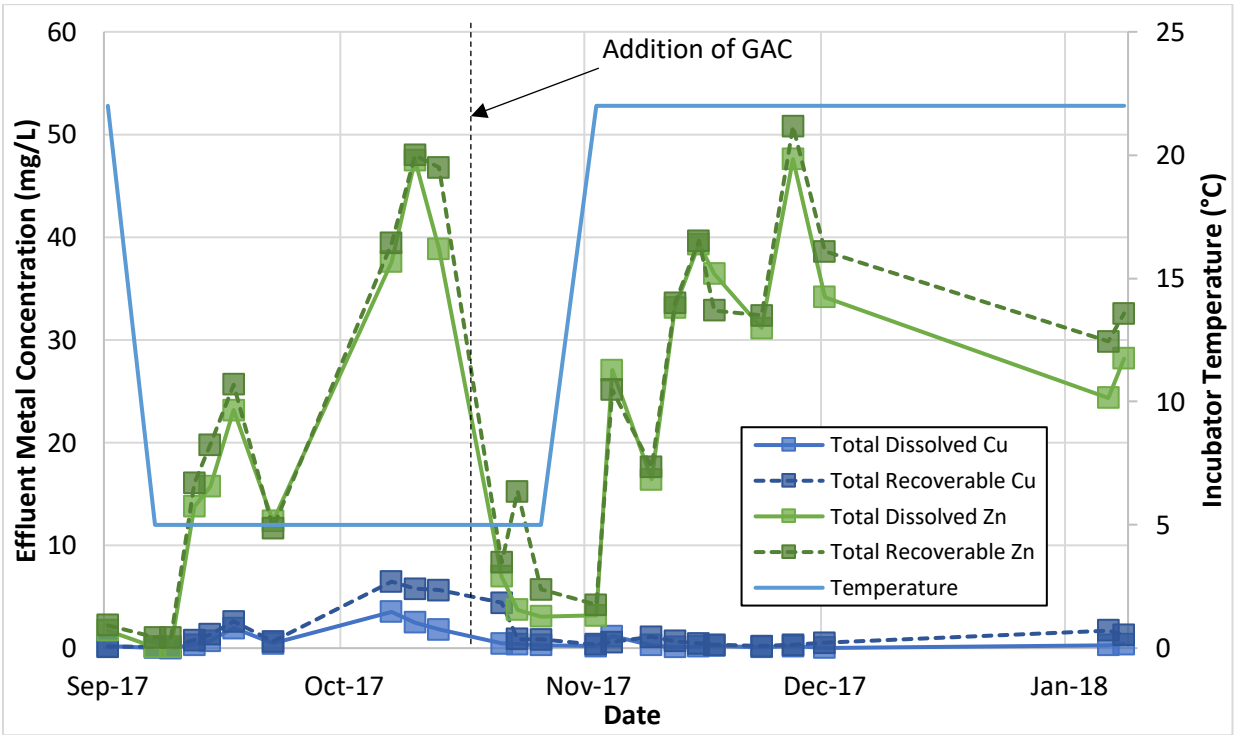


**Figure 16: SRBR effluent heavy metal concentrations (mg/L) of total recoverable and dissolved copper and zinc 09/02/2017 to 01/12/2018.**

#### 3.2.3.4. Heavy Metal Adsorption

It was evident adsorption was the responsible mechanism for heavy metal removal in the SRBR after introducing GAC to the system. Breakthrough of heavy metals occurred later than predicted. Based on the 2 kg of adsorbent added and using the adsorbent capacity determined through batch adsorption experiments, breakthrough was predicted to occur after 9 days. After the addition of GAC on 10/24/2017, it was estimated breakthrough was complete after 13 days, when heavy metal removal efficiencies began to decline and metals bypass the adsorbent.

## 3.3. Comparison of Total Recoverable and Dissolved Effluent Metals

A deviation was observed between total recoverable and dissolved copper from 11/06/2017 to 01/12/2018 – the range of time at which the incubator temperature was increased from 5°C to 22°C, and when GAC breakthrough was hypothesized to occur (Figure 16). Ten out of eleven compared effluent concentration pairs of total recoverable copper exceed dissolved copper (Figure 17). Paired copper concentrations deviate away from the 1:1 line used for reference. Contrary to copper, total recoverable zinc closely equates dissolved zinc concentrations. Paired zinc concentration values closely align with the 1:1 line (Figure 18). To investigate these deviations further, it was necessary to conduct a paired t-test to determine statistical significance.

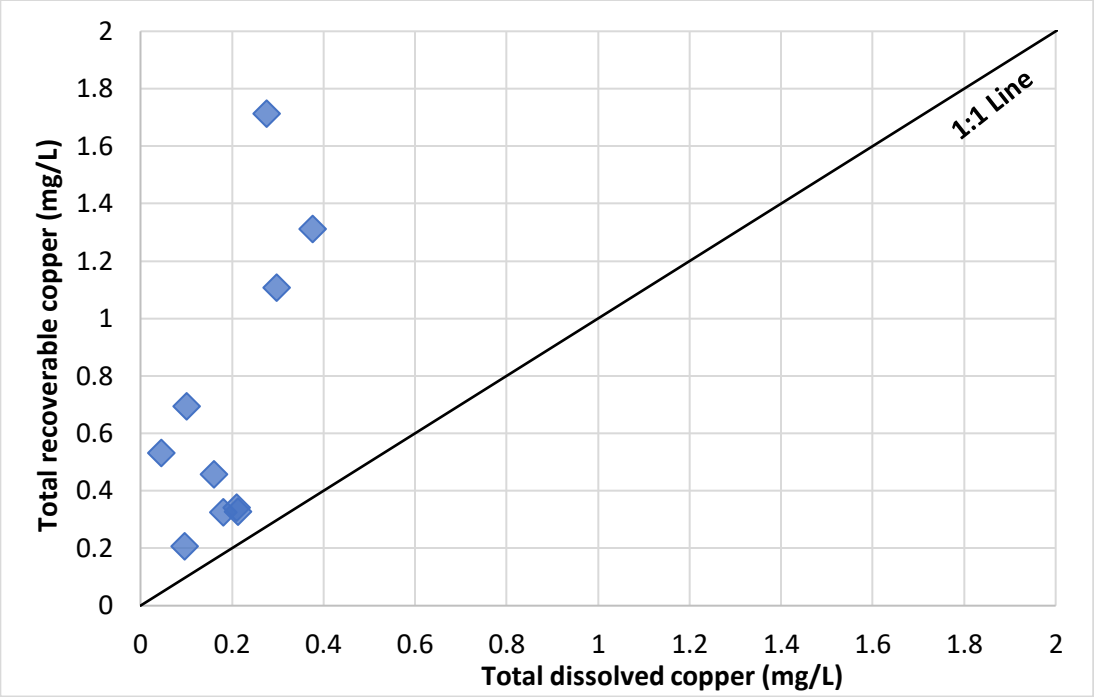


**Figure 17: SRBR effluent heavy metal concentrations of total recoverable and dissolved copper 11/06/2017 to 01/12/2018 with a 1:1 line for reference.**

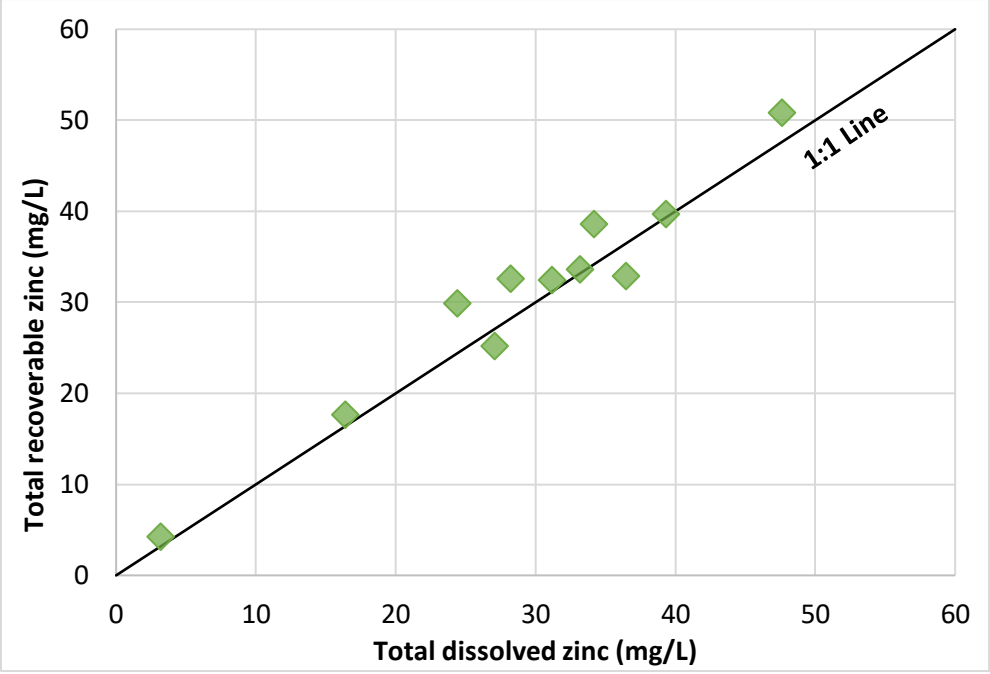


**Figure 18: SRBR effluent heavy metal concentrations of total recoverable and dissolved zinc 11/06/2017 to 01/12/2018 with a 1:1 line for reference.**

### 3.3.1. Statistical Analysis

Hypothesis testing was carried out to assess the extent of desorption of sequestered metals in the SRBR following the cold temperature cycle. Copper and zinc were separately compared using paired t-tests. The null hypothesis ($H_0$) predicted no significant difference between the mean difference ($\mu_d$) between paired total dissolved and recoverable metals concentrations. The alternative hypothesis ($H_1$) predicted a significant difference when comparing paired total recoverable and dissolved metals. Specifically, it was predicted among paired samples total dissolved metals were significantly lower than total recoverable metals. If the t statistics were lower than critical t values with significance level of 0.05, then the alternate hypothesis was accepted, and the null hypothesis rejected.

$$H_0: \mu_d = 0$$

$$H_1: \mu_d < 0$$

Based on the statistical analysis, statistical significance was found when comparing total dissolved and total recoverable effluent copper concentrations (Table X). There was a significant mean difference between paired values of total dissolved and total recoverable copper ($t$ = -3.60, $p$ = 0.00286). Therefore, the null hypothesis was rejected, and the alternate hypothesis was accepted with respect to copper.

There was no statistically significant difference between total dissolved and total recoverable zinc (Table X; $t$ = -1.77, $p$ = 0.0538). The null hypothesis was accepted, and alternate hypothesis was rejected with respect to zinc concentrations.

The Pearson correlation coefficient of total dissolved and total recoverable copper was 0.672 (Table X). A Pearson correlation coefficient value close to one indicated a strong positive correlation. Total dissolved copper was positively correlated to total recoverable copper, yet not strongly (Figure 17).

Contrary to copper, the Pearson correlation coefficient of total dissolved and total recoverable zinc was 0.974 (Table X). Total dissolved zinc was strongly correlated to total recoverable zinc. This statistic supported the linear trend observed in Figure 18.

**Table X: Paired t-test statistical comparison between dissolved and total recoverable copper and dissolved and total recoverable zinc effluent concentrations 11/06/2017 to 01/12/2018.**

| | Total Dissolved Copper | Total Recoverable Copper | Total Dissolved Zinc | Total Recoverable Zinc |
|---|---|---|---|---|
| **Mean (mg/L)** | 0.196 | 0.702 | 29.2 | 30.7 |
| **Variance (mg/L)** | 0.0103 | 0.256 | 141 | 147 |
| **Observations** | 10 | 10 | 11 | 11 |
| **Pearson Correlation** | 0.672 | | 0.974 | |
| **Hypothesized Mean Difference** | 0 | | 0 | |
| **Degrees of Freedom** | 9 | | 10 | |
| **t Statistic** | -3.60 | | -1.77 | |
| **p-value one-tail** | 0.00286 | | 0.0538 | |
| **t Critical one-tail** | 1.83 | | 1.81 | |
| **p-value two-tail** | 0.00573 | | 0.108 | |
| **t Critical two-tail** | 2.26 | | 2.23 | |

The predicted phenomenon of desorption of sequestered dissolved metals with respect to copper was supported by data and statistical analyses. Statistics did not support the occurrence of zinc desorption. These findings were best explained by selectivity of copper precipitation as opposed to zinc when in mixed solutions. The solubility product constant, $K_{sp}$, of zinc sulfide is higher than that of copper sulfide (Table XI). The higher the solubility product constant, the greater the solubility of the precipitant in water. Relative to other types of metal salts, the solubility of both copper and zinc sulfides in water are lower. For example, the solubility product constant of zinc hydroxide is $1.5 \times 10^{-23}$, which is the product of limestone addition to waters containing dissolved zinc (Lide, 2004).

**Table XI: Solubility product constants of zinc (II) sulfide and copper (II) sulfide at 25°C (Lide, 2004).**

| Reaction | Solubility Product Constant, $K_{sp}$ |
|---|---|
| $ZnS\ (s) \rightleftharpoons Zn^{2+} + S^{2-}$ | 2.0 x $10^{-25}$ |
| $CuS\ (s) \rightleftharpoons Cu^{2+} + S^{2-}$ | 8.0 x $10^{-37}$ |

After comparing solubility product constants of copper and zinc sulfides, it was reasonable to conclude that selectivity towards copper was occurring in the bioreactor. This implied excess sulfide precipitated copper ions prior to zinc ions in the form of insoluble metal sulfides. It was predicted that increased contact time and higher concentrations of excess sulfide in the bioreactor were required to precipitate sequestered zinc.

# 4. Conclusions

The first objective of this research was to compare adsorbent materials best suited to supplement an SRBR system while operating at a cold temperature with emphasis on the potential for regeneration and reuse. Second, the characterization of cold and warm temperature effects on SRBR systems was carried out. The third research objective was to determine adsorption and desorption mechanisms of the optimal adsorbent material under the influence of temperature change in the SRBR. In summary, there was success in meeting these research objectives.

## 4.1. Batch Adsorption and Desorption

After the first trial of batch adsorption and desorption experiments using GAC and NF, GAC was determined to be the suitable adsorbent material for improving SRBR cold temperature performance. Relative to GAC, twice the mass of NF (7.5 g) was required to adsorb an equivalent volume (300 mL) and concentration of copper (5 mg/L) and zinc (10 mg/L). Using GAC (3.8 g), the approximate capacity of copper and zinc in combination was 1.18 mg/g.

The first trial using GAC discovered the importance of accounting for PAC when conducting batch experiments. Nearly all the copper and zinc adsorbed to PAC, rather than GAC, with a total of 99% copper (5.41 mg/L) and 98% zinc (9.75 mg/L) adsorbed. As a result, desorption was attributed only to PAC, since heavy metals did not adsorb to GAC. Therefore, further trials were conducted with effort to remove PAC prior to adsorption. In practice, PAC cannot be introduced to a full scale SRBR for stream remediation. The goal was to attain meaningful results of desorption attributed to GAC.

Trials 2 and 3 entailed sieving and soaking GAC in DI to remove as much PAC as possible. Trial 2 was successful in demonstrating the potential for desorption of copper and zinc

with GAC (2.89 mg/L Cu, 3.22 mg/L Zn). Trial 3 was unsuccessful in removing PAC prior to desorption, but demonstrated some potential for desorption of copper and zinc from GAC.

Trials 4-6 included sieving and soaking of GAC using DI prior to adsorption, as well as decanting the adsorbate solution after adsorption was complete then replenishing with an equivalent volume of DI prior to desorption. The decanting step prior to desorption was introduced in effort to remove metals adsorbed to PAC. Desorption in Trail 4 was determined to be an outlier and results were not interpreted. Trials 5-6 demonstrated some potential for heavy metal desorption from GAC. Demonstration of desorption affirmed the occurrence of GAC regeneration by sulfide precipitation.

## 4.2. Sulfate-Reducing Bioreactor

The researched SRBR underwent several changes in operating conditions. Initially, the SRBR was operated at 22°C. The incubator temperature was reduced to 5°C starting 9/13/2017 to characterize reactor performance at a cold temperature. The selected adsorbent material, GAC, was added to the reactor on 10/24/2017 to facilitate adsorption of heavy metals. Temperature was resumed to 22°C on 11/06/2017 to characterize desorption.

### 4.2.1. Baseline Operation

Baseline operation at 22°C yielded heavy metal removal efficiencies >98% as desired sulfate reduction ranged from 282-498 mg/L. The sulfate-reduction activity was well above the minimum required 223 mg/L to precipitate the inflow dissolved copper and zinc. The zero-order sulfate reduction rate coefficient under baseline operating conditions was 0.581.

### 4.2.2. Cold Temperature Operation

The investigated SRBR system was significantly influenced by a decline in temperature to 5°C. The zero-order sulfate reduction rate coefficient at 5°C operation was 0.295. The decline

in reactor performance did not occur immediately. Within the first four days of cold temperature operation, parameters of sulfate reduction, excess sulfide, and copper and zinc removal efficiency were not significantly reduced. Throughout the remaining month of operating at 5°C in the absence of a supplementary adsorbent material, there was a decline in all metrics of reactor performance, but not a complete absence of BSR activity. Average sulfate reduction was 151 mg/L and average excess sulfide was 8 µg/L. Copper and zinc removal ranged from 88-99.98% and 52-99.91%, respectively. It was inferred that the observed freezing in the reactor towards the end of cold temperature operation had a significant effect on the rate of organic matter degradation, and thereby sulfate reduction. This study signified that an SRBR may still be employed during winter months, and would benefit from a secondary heavy metal removal mechanism.

### 4.2.3. Addition of Adsorbent

The design improvements supplemented in the SRBR were proven to be successful when sulfate reduction was inhibited in the bioreactor under 5°C conditions. A great increase in heavy metal removal was observed over a period of 13 days (91-99.09% Cu, 85-97% Zn). Effluent sulfate was impacted by GAC in the SRBR (319-489 mg/L), which was explained by adsorption of sulfate to the GAC. Excess sulfides did not change significantly after GAC was added to the bioreactor.

Following the resumption of 22°C temperature conditions, copper removal remained efficient (98-99.94%), whereas zinc removal (49-97%) did not fully recover following breakthrough of GAC. Sulfate reduction slightly increased, ranging at 176-203 mg/L. Excess sulfide concentration did not increase to former maximum levels of 15-18 µg/L, suggesting sulfide was utilized for precipitation of desorbed metals. Total dissolved copper concentrations

were significantly lower than total recoverable concentrations during this specified period of operation ($t = -3.60$, $p < 0.05$). There was no significant difference between total dissolved and total recoverable concentrations ($t = -1.77$, $p > 0.05$). Therefore, it was reasonable to conclude copper desorption by precipitation was occurring in the SRBR. It was expected zinc desorption would occur with greater excess sulfide concentrations. The selectivity could be explained by the solubility product constant of copper sulfide being lower than zinc sulfide, meaning copper sulfide precipitates more readily than zinc sulfide.

# 5. Future Work and Recommendations

The findings of this study have raised further potential research questions surrounding adsorption and desorption of heavy metals from activated carbon in a bioreactor system under the influence of temperature change.

## 5.1. Additional Cold Temperature Cycle

Strengthening the potential for long-term seasonal reuse of adsorbent following regeneration can be carried out by subjecting the SRBR to an additional cold temperature cycle. It is predicted that GAC may supplement heavy metal removal after an additional cold temperature cycle. Such an experiment should be carried out after there is adequate time for desorption of heavy metals by recreating seasonal temperature variation as much as reasonably possible. This can be achieved by waiting until the bioreactor completely returns to baseline operation under summer operating conditions.

## 5.2. Microscopic Assessment of Adsorbent Regeneration

Characterizing the surface of activated carbon following desorption of heavy metal sulfides can be conducted using a Scanning Electron Microscope (SEM). It would be valuable to compare samples of activated carbon that have not undergone adsorption (control), after adsorption of heavy metals until breakthrough, and following desorption using sulfides from the bioreactor. The available sites of activated carbon that have not undergone adsorption should be compared to adsorption sites following maximum achievable regeneration.

## 5.3. Flow-Through Adsorption-Desorption Experiments

As a lesson learned from this project, it would be beneficial to further examine the isolated effects of adsorbent regeneration in a flow-through system. In a flow-through apparatus, increased flushing of PAC from GAC granules can be achieved. It is recommended for GAC to

be positioned in a bottom-up column adsorbing heavy metals until breakthrough capacity. Once breakthrough is achieved, a solution of only sulfide ions should be fed through the system. A continuous flow of sulfide ions to desorb heavy metals from GAC may result in greater yields of desorption.

## 5.4. Alternative Adsorbent Materials

Supplementary materials with the potential to adsorb and desorb heavy metal precipitants should be further investigated. GAC was successful in adsorbing and desorbing copper, yet was inconclusive in its success of sequestering and desorbing zinc. Further research should be conducted to find an adsorbent material that has an affinity towards zinc in mixed solutions. Since the effects of GAC on reactor performance are known, a second material may be added inside the reactor to enhance zinc removal.

## 5.5. Grove Gulch Pilot Reactor Study

After the success of supplementing a bench-scale SRBR with GAC operating under winter-time conditions, it is recommended that a pilot-scale reactor study be implemented at Grove Gulch. Based on prior investigation of sources of heavy metal contamination, the full-scale SRBR should be located directly before Grove Gulch waters flow into Blacktail Creek (Craig, 2016). Based on bench-scale studies, implementing a single-phase SRBR system containing limestone would yield approximately 52-99% removal of heavy metals during the winter months (5°C). Using an adsorbent, such as GAC, this performance may be improved.

At a full scale, it is recommended to use a two-stage system. The first stage being the SRBR and the second stage being GAC. It is suggested that the activated carbon be placed in series following the SRBR, rather than inside of the SRBR. Best efforts should be made to avoid loss of sulfides prior to contact with the adsorbent. Loss of sulfides can occur by escaping

hydrogen sulfide through a gas vent. If plausible, gas should not be vented until after contact with sequestered dissolved metals on the adsorbent. The mechanism driving desorption is contact of adsorbed dissolved metals with excess sulfides.

During the first winter, a significant increase in reactor performance is anticipated, mainly explained by adsorption (approximately 85-99%). The following summer, it is expected that GAC would be regenerated for the next cold-temperature cycle (using batch experiment measurements, varying 14-91%) use. Since regeneration of GAC cannot be achieved in complete, winter-time performance in the subsequent cold cycle would not be as efficient as the initial cycle following GAC implementation. An overall improvement in long-term SRBR performance is anticipated with seasonally-regenerated GAC relative to a system without a design modification. Further long-term studies are required to quantify the heavy metal removal efficiency after subsequent cold temperature cycles following GAC regeneration in the summer months.

# 6. References Cited

Akcil, A., & Koldas, S. (2006). Acid Mine Drainage (AMD): causes, treatment and case studies. *Journal of Cleaner Production, 14*(12), 1139-1145.

Brown, D. E., Groves, G. R., & Miller, J. D. (1973). pH and Eh control of cultures of sulphate-reducing bacteria. *Journal of Chemical Technology and Biotechnology, 23*(2), 141-149.

Cohen, R. R. (2006). Use of microbes for cost reduction of metal removal from metals and mining industry waste streams. *Journal of Cleaner Production, 14*, 1146-1157.

Craig, G. (2016). *Characterizing Sources of Nutrient Loading and Heavy Metals and Developing Best Management Practices for Grove Gulch in Butte, MT.* Master's Thesis, Montana Tech of the University of Montana, Department of Environmental Engineering.

Crittenden, J. C., Rhodes Trussell, R., Hand, D. W., Howe, K. J., & Tchobanoglous, G. (2012). *MWH's Water Treatment: Principles and Design* (3rd Edition ed.). Hoboken, NJ: John Wiley & Sons.

Dev, S., Roy, S., & Bhattacharya, J. (2017). Optimization of the operation of packed bed bioreactor to improve the sulfate and metal removal from acid mine drainage. *Journal of Environmental Management, 200*, 135-144.

Drury, W. J. (1999). Treatment of acid mine drainage with anaerobic solid-substrate reactors. *Water Environment Research, 71*(6), 1244-1250.

Drury, W. J. (2000). Modeling of sulfate reduction in anaerobic solid substrate bioreactors for mine drainage treatment. *Mine Water and the Environment, 19*(1), 19-29.

Drury, W. J. (2017). Memo on Zero-Order Model. *Personal Communication*.

Duaime, T. E., Metesh, J. J., Bergantino, R. N., Burns, G., Yovich, M. J., Lee-Roark, C. L., . . . Ford, J. F. (1995). Hydrologic aspects of remediation of metal mine impacts on Upper Clark Fork Superfund sites, Butte-Warm Springs, MT. *Northwest Geology, 24*, 99-158.

Duaime, T., Sonderegger, J., & Zaluski, M. (1985). Hydrogeology of the Colorado Tailings Area, Butte, MT. *Proceedings of the Clark Fork River Symposium* (p. 420). Butte, MT: Montana College of Mineral Science and Technology.

Dumbrava, A., Ciupina, V., & Prodan, G. (2005). Dependence of grain size and morphology of zinc sulfide particles by the synthesis route. *Romanian Journal of Physics, 50*, 831-836.

Dvorak, D. H., Hedin, R. S., Edenborn, H. M., & McIntire, P. E. (1992). Treatment of metal-contaminated water using bacterial sulfate reduction: results from pilot-scale reactors. *Biotechnology and Bioengineering, 40*(5), 609-616.

Eger, P. (1992). The use of sulfate reduction to remove metals from acid mine drainage. *America Society of Mining and Reclamation*, (pp. 563-576). Duluth, MN.

Gammons, C. H., & Frandsen, A. K. (2001). Fate and transport of metals in H2S-rich waters at a treatment wetland. *Geochem. Trans., 2*(1), 1-15.

Gammons, C. H., Mulholland, T. P., & Frandsen, A. K. (2000). A comparison of filtered vs. unfiltered metal concentrations in treatment wetlands. *Mine Water and the Environment, 19*, 111-123.

Gammons, C. H., Shope, C. L., & Duaime, T. E. (2005). A 24h investigation of the hydrogeochemistry of baseflow and stormwater in an urban area impacted by mining: Butte, Montana. *Hydrological Processes, 19*, 2737-2753.

Gusek, J. J. (2000). Reality check: passive treatment of mine drainage an emerging technology or proven methodology? *SME Annual Meeting.* Salt Lake City, Utah.

Gusek, J. J. (2004). Scaling up design challenges for large scale sulfate reducing bioreactors. *Proceedings American Society of Mining and Reclamation.* Lexington, KY: ASMR.

Gusek, J. J., & Wildeman, T. R. (2002). Passive treatment of aluminum-bearing acid rock drainage. *23rd Annual West Virginia Surface Mine Drainage Task Force Symposium.* Morgantown, WV.

Janin, A., & Harrington, J. (2015). Performances of lab-scale anaerobic bioreactors at low temperature using Yukon native microorganisms. *Proceedings of Mine Water Solutions in Extreme Environments*, 519-532.

Lide, D. R. (2004). *CRC Handbook of Chemistry and Physics.* Portland, OR: CRC Press.

Lindsay, M. B., Moncur, M. C., Bain, J. G., Jambor, J. L., Ptacek, C. J., & Blowes, D. W. (2015). Geochemical and mineralogical aspects of sulfide mine tailings. *Applied Geochemistry, 57*, 157-177.

Machemer, S. D., & Wildeman, T. R. (1992). Adsorption compared with sulfide precipitation as metal removal processes from acid mine drainage in a constructed wetland. *Journal of Contaminant Hydrogeology, 9*, 115-131.

Montana Department of Environmental Quality. (2012). *Montana Numeric Water Quality Standards.* Helena, MT.

Montana Department of Labor & Industry. (2014). *Montana Economy at a Glance.*

Mugisidi, D., Ranaldo, A., Soedarsono, J. W., & Muhammad, H. (2007). Modification of activated carbon using sodium acetate and its regeneration using sodium hydroxide for the adsorption of copper from aqueous solution. *Carbon, 45*, 1081-1084.

Namasivayam, D. S. (2008). Coconut coir pith for removal of sulfate. *Journal of Desalination, 219*, 1-13.

Neculita, C.-M., Zagury, G. J., & Bussière, B. (2007). Passive treatment of acid mine drainage in bioreactors using sulfate-reducing bacteria: critical review and research needs. *Journal of Environmental Quality, 36*(1), 1-16.

Postgate, J. R. (1984). *The Sulfate-Reducing Bacteria* (2nd Edition ed.). Cambridge, UK: Cambridge University Press.

Ribet, I., Ptacek, C. J., Blowes, D. W., & Jambor, J. L. (1995). The potential for metal release by reductive dissolution of weathered mine tailings. *Journal of Contaminant Hydrology, 17*(3), 239-273.

Salmon, M. S. (2009). Removal of sulfate from waste water by activated carbon. *Al-Khwarizmi Engineering Journal, 5*(3), 72-76.

Stumm, W., & Morgan, J. J. (1981). *Aquatic Chemistry* (2nd Edition ed.). New York: John Wiley & Sons.

Tank, N. S., Parikh, K. D., & Joshi, M. J. (2017). Synthesis and characterization of copper sulphide (CuS) nano particles. *AIP Conference Proceedings. 1837.* AIP Publishing.

Tripetchkul, S., Pundee, K., Koonsrisuk, S., & Akeprathumchai, S. (2012). Co-composting of coir pith and cow manure: initial C/N ratio vs physico-chemical changes. *International Journal of Recycling of Organic Waste in Agriculture, 1*(15), 1-8.

Tsukamoto, T. K., Killion, H. A., & Miller, G. C. (2004). Column experiments for microbiological treatment of acid mine drainage: low-temperature, low-pH and matrix investigations. *Water Research, 38*, 1405-1418.

United States Environmental Protection Agency. (2006). *Record of Decision.* Butte Priority Soils Operable Unit, Silver Bow Creek/Butte Area NPL Site, Butte, MT.

United States Environmental Protection Agency. (2014). *Reference Guide to Treatment Technologies for Mining-Influenced Water.*

United States Environmental Protection Agency. (2015). *Interim Record of Decision for the Bullion Mine.* Jefferson County, MT.

United States Environmental Protection Agency. (2016). *Fourth Five-Year Report for Silver Bow Creek/Butte Area Superfund Site.*

Willow, M. A., & Cohen, R. R. (2003). pH, dissolved oxygen, and adsorption effects on anaerobic bioreactors. *J. Environ. Qual., 32*(4), 1212-1221.

# 7. Appendix A: Batch Adsorption-Desorption Sample Mass Balances

For each trial of batch adsorption-desorption experiments, copper and zinc mass balances were employed to assess the success of each trial (Eqns 10-17). All trials held the assumption of steady state, with metals in equal to metals out inside each flask. Trials 1-3 mass balances were all conducted in the same manner, accounting for PAC desorbed. Trials 2 and 5 mass balance calculations were decomposed into example calculations (Figure 19; Figure 20). Trials 4-6 mass balances were conducted in the same manner, except it was assumed PAC was no longer a contributing factor when flasks were decanted after adsorption.

## 7.1. Trial 2

| **TRIAL 2 GAC** | ICP Output | | **Dilution Factor Applied** | | Comment |
|---|---|---|---|---|---|
| Samples | Cu (mg/L) | Zn (mg/L) | **Cu (mg/L)** | **Zn (mg/L)** | |
| GAC-101117-1 | 0.9034 | 2.044 | **1.8068** | **4.088** | Total recoverable metals concentration after 24 h adsorption |
| DGAC-101117-1 | 0.1006 | 0.2229 | **0.2012** | **0.4458** | Total dissolved metals concentration after 24 h adsorption |
| GAC-101117-2 | 2.351 | 3.654 | **4.702** | **7.308** | Total recoverable metals after desorbed with Na2S over 24 hours |
| DGAC-101117-2 | 0.5209 | 0.4199 | **1.0418** | **0.8398** | Total dissolved metals after desorbed with Na2S over 24 hours |
| Initial Concentrations | | | 5 | 10 | |
| | | | | | |
| | | | | | |
| **Adsorption** | Copper | Zinc | | | |
| Adsorbed to GAC | 3.1932 | 5.912 | | | |
| Adsorbed to PAC | 1.6056 | 3.6422 | | | |
| **TOTAL ADSORBED** | 4.7988 | 9.5542 | | | |
| | | | | | |
| **Desorption** | | | | | |
| Desorbed from GAC | 2.8952 | 3.22 | | | |
| | | | | | |
| | | | | | |
| | | | | | |
| | | | | | |
| Remaining on GAC | 0.298 | 2.692 | | | |
| **PERCENT DESORBED FROM GAC** | **90.7%** | **54.5%** | | | |

**Figure 19: Trial 2 adsorption-desorption batch experiment mass balance summary.**

### 7.1.1. Copper

#### 7.1.1.1. Adsorption

*Total Cu Adsorbed = Initial Cu Adsorbate Input – Total Dissolved Cu after Adsorption*

*Total Cu Adsorbed = 5 mg/L – 0.2012 mg/L = 4.7988 mg/L*

*Total Cu Adsorbed = Cu Adsorbed to PAC + Cu Adsorbed to GAC*

*Cu Adsorbed to PAC = Total Recoverable Cu after Adsorption – Total Dissolved Cu*

*Cu Adsorbed to PAC = 1.8068 mg/L – 0.2012 mg/L = 1.6056 mg/L*

*Cu Adsorbed to GAC = Total Cu Adsorbed – Cu Adsorbed to PAC*

*Cu Adsorbed to GAC = 4.7988 mg/L – 1.6056 mg/L = 3.1932 mg/L*

$$\textit{Fraction of Cu Adsorbed} = \frac{\textit{Total Cu Adsorbed}}{\textit{Initial Cu Adsorbate Input}} = \frac{4.7988\ mg/L}{5\ mg/L} = 96\%$$

#### 7.1.1.2. Desorption

| | | | | |
|---|---|---|---|---|
| *Total Cu Desorbed from GAC* | = | *Total Recoverable Cu after Desorption* | – | *Total Recoverable Cu after Adsorption* |

*Total Cu Desorbed from GAC = 4.702 mg/L – 1.8068 mg/L = 2.8952 mg/L*

$$\textit{Fraction of Cu Desorbed from GAC} = \frac{\textit{Total Cu Desorbed from GAC}}{\textit{Total Cu Adsorbed to GAC}} = \frac{2.8952\ mg/L}{3.1932\ mg/L} = 90.7\%$$

### 7.1.2. Zinc

#### 7.1.2.1. Adsorption

*Total Zn Adsorbed = Initial Zn Adsorbate Input – Total Dissolved Zn after Adsorption*

*Total Zn Adsorbed = 10 mg/L – 0.4458 mg/L = 9.5542 mg/L*

*Total Zn Adsorbed = Zn Adsorbed to PAC + Zn Adsorbed to GAC*

*Zn Adsorbed to PAC = Total Recoverable Zn after Adsorption – Total Dissolved Zn*

*Zn Adsorbed to PAC = 4.088 mg/L – 0.4458 mg/L = 3.6422 mg/L*

*Zn Adsorbed to GAC = Total Zn Adsorbed – Zn Adsorbed to PAC*

*Zn Adsorbed to GAC = 9.5542 mg/L – 3.6422 mg/L = 5.912 mg/L*

$$\textit{Fraction of Zn Adsorbed} = \frac{\textit{Total Zn Adsorbed}}{\textit{Initial Zn Adsorbate Input}} = \frac{9.5542\ mg/L}{10\ mg/L} = 96\%$$

#### 7.1.2.2. Desorption

| | | | | |
|---|---|---|---|---|
| *Total Zn Desorbed from GAC* | = | *Total Recoverable Zn after Desorption* | – | *Total Recoverable Zn after Adsorption* |

$$Total\ Zn\ Desorbed\ from\ GAC = 7.308\ mg/L - 4.088\ mg/L = 3.220\ mg/L$$

$$Fraction\ of\ Zn\ Desorbed\ from\ GAC = \frac{Total\ Zn\ Desorbed\ from\ GAC}{Total\ Zn\ Adsorbed\ to\ GAC} = \frac{3.220\ mg/L}{5.912\ mg/L} = 54.5\ \%$$

## 7.2. Trial 5

| TRIAL 5 GAC | ICP Output | | Dilution Factor Applied | | |
|---|---|---|---|---|---|
| Samples | Cu (mg/L) | Zn (mg/L) | Cu (mg/L) | Zn (mg/L) | |
| GAC-111317-R2-1 | 0.7757 | 1.864 | **2.586** | **6.213** | Total recoverable 24 h after adsorption |
| DGAC-111317-R2-1 | 0.3415 | 1.787 | **0.854** | **4.468** | Total dissolved 24 h after adsorption |
| GAC-111317-R2-2 | 0.2291 | 0.3371 | **0.458** | **0.674** | Total recoverable 24 h after desorption and decanting. |
| DGAC-111317-R2-2 | 0.0702 | 0.1604 | **0.140** | **0.321** | Total dissolved 24 h after desorption and decanting. |
| | | | | | |
| Initial Concentrations | | | 5 | 10 | |
| | | | | | |
| | | | | | |
| | | | | | |
| | Copper | Zinc | | | |
| Adsorbed to GAC | 2.414 | 3.787 | | | |
| Adsorbed to PAC | 1.732 | 1.746 | | | |
| Total adsorbed | 4.146 | 5.533 | | | |
| | | | | | |
| Desorbed from GAC | 0.458 | 0.674 | | | |
| | | | | | |
| | | | | | |
| | | | | | |
| | | | | | |
| Remaining on GAC | 1.956 | 3.112 | | | |
| **Percent Desorbed from GAC** | **19.0%** | **17.8%** | | | |

**Figure 20: Trial 5 adsorption-desorption batch experiment mass balance summary.**

### 7.2.1. Copper

#### 7.2.1.1. Adsorption

*Total Cu Adsorbed = Initial Cu Adsorbate Input – Total Dissolved Cu after Adsorption*

*Total Cu Adsorbed = 5 mg/L – 0.854 mg/L = 4.146 mg/L*

*Total Cu Adsorbed = Cu Adsorbed to PAC + Cu Adsorbed to GAC*

*Cu Adsorbed to PAC = Total Recoverable Cu after Adsorption – Total Dissolved Cu*

*Cu Adsorbed to PAC = 2.586 mg/L – 0.854 mg/L = 1.732 mg/L*

*Cu Adsorbed to GAC = Total Cu Adsorbed – Cu Adsorbed to PAC*

*Cu Adsorbed to GAC = 4.146 mg/L – 1.732 mg/L = 2.414 mg/L*

$$Fraction\ of\ Cu\ Adsorbed = \frac{Total\ Cu\ Adsorbed}{Initial\ Cu\ Adsorbate\ Input} = \frac{4.146\ mg/L}{5\ mg/L} = 82.9\%$$

#### 7.2.1.2. Desorption

| | | |
|---|---|---|
| *Total Cu Desorbed from GAC* | = | *Total Recoverable Cu after Desorption* |

$$Total\ Cu\ Desorbed\ from\ GAC = 0.458\ mg/L$$

$$Fraction\ of\ Cu\ Desorbed\ from\ GAC = \frac{Total\ Cu\ Desorbed\ from\ GAC}{Total\ Cu\ Adsorbed\ to\ GAC} = \frac{0.458\ mg/L}{2.414\ mg/L} = 19.0\%$$

### 7.2.2. Zinc

#### 7.2.2.1. Adsorption

$$Total\ Zn\ Adsorbed = Initial\ Zn\ Adsorbate\ Input - Total\ Dissolved\ Zn\ after\ Adsorption$$

$$Total\ Zn\ Adsorbed = 10\ mg/L - 4.468\ mg/L = 5.533\ mg/L$$

$$Total\ Zn\ Adsorbed = Zn\ Adsorbed\ to\ PAC + Zn\ Adsorbed\ to\ GAC$$

$$Zn\ Adsorbed\ to\ PAC = Total\ Recoverable\ Zn\ after\ Adsorption - Total\ Dissolved\ Zn$$

$$Zn\ Adsorbed\ to\ PAC = 6.213\ mg/L - 4.468\ mg/L = 1.746\ mg/L$$

$$Zn\ Adsorbed\ to\ GAC = Total\ Zn\ Adsorbed - Zn\ Adsorbed\ to\ PAC$$

$$Zn\ Adsorbed\ to\ GAC = 5.533\ mg/L - 1.746\ mg/L = 3.787\ mg/L$$

$$Fraction\ of\ Zn\ Adsorbed = \frac{Total\ Zn\ Adsorbed}{Initial\ Zn\ Adsorbate\ Input} = \frac{5.533\ mg/L}{10\ mg/L} = 55.3\%$$

#### 7.2.2.2. Desorption

| | | |
|---|---|---|
| *Total Zn Desorbed from GAC* | = | *Total Recoverable Zn after Desorption* |

$$Total\ Zn\ Desorbed\ from\ GAC = 0.674\ mg/L$$

$$Fraction\ of\ Zn\ Desorbed\ from\ GAC = \frac{Total\ Zn\ Desorbed\ from\ GAC}{Total\ Zn\ Adsorbed\ to\ GAC} = \frac{0.674\ mg/L}{3.787\ mg/L} = 17.8\%$$

# 8. Appendix B: Adsorbent Breakthrough Estimation

## 8.1. Preliminary Batch Adsorption

For simplification of estimating breakthrough, adsorbate concentrations in batch experiments were simplified to 15 mg/L of total divalent metals. A mass of 3.8 grams of GAC after sieving was used for batch adsorption experiments. The approximate breakthrough capacity of the GAC used was determined using the ratio (mg/g) of the mass of adsorbate (mg) to adsorbent (g). As a result, the capacity of GAC was approximately 1.18 mg/g.

$$Adsorption\ Capacity = \frac{adsorbate\ mass}{adsorbent\ mass} = \frac{15\frac{mg}{L}\ Me^{2+} * 0.300\ L}{3.8\ g\ GAC} = 1.18\frac{mg\ Me^{2+}}{g\ GAC}$$

## 8.2. Sulfate-Reducing Bioreactor Breakthrough

The breakthrough capacity determined through batch adsorption was used to estimate the time of breakthrough based on mass loadings inside the SRBR. The greatest drop in efficiency over 5°C operation resulted in a total recoverable effluent divalent metals concentration of about 50 mg/L. The highest effluent metals concentration and reactor flow rate (3.8 mL/min) were used to estimate the breakthrough time at which 2 kg of GAC were to be completely spent inside the SRBR.

$$Me^{2+}Mass\ Flow\ Rate = 50\frac{mg}{L}\ Me^{2+} * 3.8\frac{mL}{min} * \frac{L}{1000\ mL} * \frac{60*24\ min}{d} = 273.6\ \frac{mg\ Me^{2+}}{d}$$

$$Breakthrough\ Time = \frac{d}{273.6\ mg\ Me^{2+}} * 1.18\ \frac{mg\ Me^{2+}}{g\ GAC} * 2000\ g\ GAC = 9\ days$$

# 9. Appendix C: Sulfate-Reducing Bioreactor Experimental Data

**Table XII: Bioreactor dissolved effluent concentrations and removal efficiencies of copper and zinc 09/05/2017 to 01/12/2018.**

| Date Sampled | Dissolved Cu (mg/L) | Dissolved Zn (mg/L) | Sum of Dissolved Metals (mg/L) | Dissolved Cu Efficiency | Dissolved Zn Efficiency | Total Removal Efficiency |
|---|---|---|---|---|---|---|
| 2017-09-05 | 0.206 | 1.71 | 1.92 | 99.6% | 98.3% | 98.7% |
| 2017-09-11 | 0.0189 | 0.103 | 0.122 | 99.96% | 99.9% | 99.9% |
| 2017-09-13 | 0.00910 | 0.0904 | 0.0995 | 99.98% | 99.9% | 99.9% |
| 2017-09-16 | 0.314 | 13.8 | 14.1 | 99.4% | 86.2% | 90.6% |
| 2017-09-18 | 0.715 | 15.7 | 16.5 | 98.6% | 84.3% | 89.0% |
| 2017-09-21 | 1.95 | 23.2 | 25.1 | 96.1% | 76.8% | 83.2% |
| 2017-09-26 | 0.454 | 12.4 | 12.8 | 99.1% | 87.6% | 91.4% |
| 2017-10-05 | 2.79 | 28.1 | 30.9 | 94.4% | 71.9% | 79.4% |
| 2017-10-11 | 3.53 | 37.6 | 41.1 | 92.9% | 62.4% | 72.6% |
| 2017-10-14 | 2.50 | 47.5 | 50.0 | 95.0% | 52.5% | 66.7% |
| 2017-10-17 | 1.82 | 38.9 | 40.7 | 96.4% | 61.1% | 72.9% |
| 2017-10-25 | 0.456 | 6.99 | 7.44 | 99.1% | 93.0% | 95.0% |
| 2017-10-27 | 0.398 | 3.73 | 4.13 | 99.2% | 96.3% | 97.3% |
| 2017-10-30 | 0.282 | 3.08 | 3.36 | 99.4% | 96.9% | 97.8% |
| 2017-11-06 | 0.210 | 3.18 | 3.39 | 99.6% | 96.8% | 97.7% |
| 2017-11-08 | 1.17 | 27.1 | 28.2 | 97.7% | 72.9% | 81.2% |
| 2017-11-13 | 0.297 | 16.4 | 16.7 | 99.4% | 83.6% | 88.9% |
| 2017-11-16 | 0.101 | 33.2 | 33.3 | 99.8% | 66.8% | 77.8% |
| 2017-11-19 | 0.160 | 39.3 | 39.5 | 99.7% | 60.7% | 73.7% |
| 2017-11-21 | 0.213 | 36.4 | 36.7 | 99.6% | 63.6% | 75.6% |
| 2017-11-27 | 0.0966 | 31.2 | 31.3 | 99.8% | 68.8% | 79.2% |
| 2017-12-01 | 0.182 | 47.6 | 47.8 | 99.6% | 52.4% | 68.1% |
| 2017-12-05 | 0.046 | 34.2 | 34.2 | 99.9% | 65.8% | 77.2% |
| 2018-01-10 | 0.276 | 24.4 | 24.7 | 99.4% | 75.6% | 83.6% |
| 2018-01-12 | 0.377 | 28.2 | 28.6 | 99.2% | 71.8% | 80.9% |

**Table XIII: Bioreactor total recoverable effluent concentrations and removal efficiencies of copper and zinc 09/05/2017 to 01/12/2018.**

| Date Sampled | Total Recoverable Cu (mg/L) | Total Recoverable Zn (mg/L) | Sum of Total Recoverable Metals (mg/L) | Total Recoverable Cu Efficiency | Total Recoverable Zn Efficiency | Total Removal Efficiency |
|---|---|---|---|---|---|---|
| 2017-09-05 | 0.133 | 2.24 | 2.37 | 99.7% | 97.8% | 98.4% |
| 2017-09-11 | 0.117 | 1.05 | 1.16 | 99.8% | 99.0% | 99.2% |
| 2017-09-13 | 0.115 | 1.03 | 1.14 | 99.8% | 99.0% | 99.2% |
| 2017-09-16 | 0.785 | 16.1 | 16.9 | 98.4% | 83.9% | 88.8% |
| 2017-09-18 | 1.32 | 19.8 | 21.1 | 97.4% | 80.2% | 85.9% |
| 2017-09-21 | 2.59 | 25.7 | 28.3 | 94.8% | 74.3% | 81.2% |
| 2017-09-26 | 0.635 | 11.7 | 12.3 | 98.7% | 88.3% | 91.8% |
| 2017-10-02 | 3.70 | 21.7 | 25.4 | 92.6% | 78.3% | 83.1% |
| 2017-10-11 | 6.48 | 39.4 | 45.9 | 87.0% | 60.6% | 69.4% |
| 2017-10-14 | 5.77 | 48.0 | 53.8 | 88.5% | 52.0% | 64.2% |
| 2017-10-17 | 5.66 | 46.8 | 52.4 | 88.7% | 53.2% | 65.0% |
| 2017-10-25 | 4.41 | 8.35 | 12.8 | 91.2% | 91.7% | 91.5% |
| 2017-10-27 | 0.875 | 15.27 | 16.1 | 98.3% | 84.7% | 89.2% |
| 2017-10-30 | 0.830 | 5.72 | 6.55 | 98.3% | 94.3% | 95.6% |
| 2017-11-06 | 0.342 | 4.21 | 4.55 | 99.3% | 95.8% | 97.0% |
| 2017-11-08 | 0.587 | 25.1 | 25.7 | 98.8% | 74.9% | 82.8% |
| 2017-11-13 | 1.11 | 17.6 | 18.7 | 97.8% | 82.4% | 87.5% |
| 2017-11-16 | 0.694 | 33.6 | 34.3 | 98.6% | 66.4% | 77.1% |
| 2017-11-19 | 0.456 | 39.6 | 40.1 | 99.1% | 60.4% | 73.3% |
| 2017-11-21 | 0.328 | 32.9 | 33.2 | 99.3% | 67.1% | 77.9% |
| 2017-11-27 | 0.208 | 32.4 | 32.6 | 99.6% | 67.6% | 78.3% |
| 2017-12-01 | 0.326 | 50.8 | 51.1 | 99.3% | 49.2% | 65.9% |
| 2017-12-05 | 0.531 | 38.6 | 39.1 | 98.9% | 61.4% | 73.9% |
| 2018-01-10 | 1.71 | 29.9 | 31.6 | 96.6% | 70.1% | 79.0% |
| 2018-01-12 | 1.31 | 32.6 | 33.9 | 97.4% | 67.4% | 77.4% |

**Table XIV: Bioreactor measured influent and effluent sulfate concentrations, change in sulfate, and fraction of sulfate 04/05/2017 to 01/24/2018. Starred values indicate assumed $S_0$ = 1300 mg/L. Change in sulfate and fraction of sulfate calculated using $S_0$ = 1300 mg/L.**

| Date Sampled | Temperature (°C) | Measured Influent Sulfate (mg $SO_4^{2-}$/L) | Effluent Sulfate, S (mg $SO_4^{2-}$/L) | Sulfate Reduction $S_0 - S$ (mg $SO_4^{2-}$/L); $S_0$=1300 mg/L | $S/S_0$ |
|---|---|---|---|---|---|
| 2017-04-05 | 22 | 1320 | 900 | 400 | 0.692 |
| 2017-04-06 | 22 | 1390 | 954 | 346 | 0.734 |
| 2017-04-10 | 22 | 1256 | 953 | 347 | 0.733 |
| 2017-04-20 | 22 | 1346 | 802 | 498 | 0.617 |
| 2017-04-24 | 22 | 1219 | 911 | 389 | 0.701 |
| 2017-05-11 | 22 | 1300* | 878 | 422 | 0.675 |
| 2017-05-17 | 22 | 1300* | 988 | 312 | 0.760 |
| 2017-05-24 | 22 | 1300* | 971 | 329 | 0.747 |
| 2017-06-02 | 22 | 1300* | 912 | 388 | 0.702 |
| 2017-06-07 | 22 | 1300* | 935 | 365 | 0.719 |
| 2017-06-15 | 22 | 1300* | 976 | 324 | 0.751 |
| 2017-06-21 | 22 | 1300* | 961 | 339 | 0.739 |
| 2017-07-07 | 22 | 1300* | 1018 | 282 | 0.783 |
| 2017-07-21 | 22 | 1300* | 982 | 318 | 0.755 |
| 2017-08-07 | 22 | 1300* | 976 | 324 | 0.751 |
| 2017-09-05 | 22 | 1300* | 818 | 482 | 0.629 |
| 2017-09-11 | 22 | 1261 | 870 | 430 | 0.669 |
| 2017-09-13 | 5 | 1261 | 833 | 467 | 0.641 |
| 2017-09-16 | 5 | 1269 | 1180 | 120 | 0.908 |
| 2017-09-18 | 5 | 1246 | 1167 | 133 | 0.898 |
| 2017-09-21 | 5 | 1256 | 1153 | 148 | 0.887 |
| 2017-09-26 | 5 | 1260 | 1140 | 160 | 0.877 |
| 2017-10-02 | 5 | 1270 | 1155 | 145 | 0.888 |
| 2017-10-05 | 5 | 1270 | 1246 | 54 | 0.958 |
| 2017-10-09 | 5 | 1224 | 1202 | 98 | 0.925 |
| 2017-10-14 | 5 | 1222 | 1219 | 81 | 0.938 |
| 2017-10-17 | 5 | 1222 | 1196 | 104 | 0.920 |
| 2017-10-25 | 5 | 1261 | 811 | 489 | 0.624 |
| 2017-10-27 | 5 | 1247 | 884 | 416 | 0.680 |
| 2017-10-30 | 5 | 1287 | 909 | 391 | 0.699 |
| 2017-11-06 | 22 | 1225 | 981 | 319 | 0.755 |
| 2017-11-08 | 22 | 1236 | 1167 | 133 | 0.898 |
| 2017-11-13 | 22 | 1240 | 1140 | 160 | 0.877 |
| 2017-11-16 | 22 | 1310 | 1204 | 96 | 0.926 |
| 2017-11-19 | 22 | 1250 | 1171 | 129 | 0.901 |

| | | | | | |
|---|---|---|---|---|---|
| 2017-11-21 | 22 | 1250 | 1174 | 126 | 0.903 |
| 2017-11-27 | 22 | 1250 | 1141 | 159 | 0.878 |
| 2017-12-01 | 22 | 1250 | 1171 | 130 | 0.900 |
| 2017-12-05 | 22 | 1321 | 1171 | 129 | 0.901 |
| 2018-01-10 | 22 | 1333 | 1097 | 203 | 0.844 |
| 2018-01-12 | 22 | 1255 | 1124 | 176 | 0.865 |
| 2018-01-24 | 22 | 1277 | 1112 | 188 | 0.855 |

**Table XV: Bioreactor dissolved effluent sulfide concentrations (µg $S^{2-}$/L) 09/21/2017 to 01/24/2018.**

| Date | Effluent Dissolved Sulfide (µg $S^{2-}$/L) |
|---|---|
| September 21, 2017 | 14 |
| September 26, 2017 | 18 |
| October 2, 2017 | 7 |
| October 5, 2017 | 7 |
| October 9, 2017 | 9 |
| October 11, 2017 | 8 |
| October 14, 2017 | 8 |
| October 17, 2017 | 7 |
| October 20, 2017 | 8 |
| October 25, 2017 | 7 |
| October 27, 2017 | 7 |
| October 30, 2017 | 6 |
| November 6, 2017 | 7 |
| November 8, 2017 | 5 |
| November 13, 2017 | 7 |
| November 16, 2017 | 6 |
| November 19, 2017 | 5 |
| November 21, 2017 | 7 |
| November 27, 2017 | 7 |
| December 1, 2017 | 7 |
| December 5, 2017 | 8 |
| January 10, 2018 | 6 |
| January 12, 2018 | 6 |
| January 24, 2018 | <MDL |

# 10. Appendix D: Sulfate Reduction Sample Calculations

The overall reaction representing precipitation of heavy metals mediated by sulfate reduction was described in Eqn. (5). Using stoichiometry, the minimum required change in effluent sulfate was predicted.

Required sulfate concentration to precipitate zinc ions:

$$\Delta S_{Zn} = 100\frac{mg}{L}\ Zn^{2+} * \frac{mmol}{65.38\ mg\ Zn} * \frac{1\ mmol\ SO_4^{2-}}{1\ mmol\ Zn^{2+}} * \frac{96.06\ mg\ SO_4^{2-}}{mmol} = 146.9\frac{mg}{L}\ SO_4^{2-}$$

Required sulfate concentration to precipitate copper ions:

$$\Delta S_{Cu} = 50\frac{mg}{L}\ Zn^{2+} * \frac{mmol}{63.55\ mg\ Zn} * \frac{1\ mmol\ SO_4^{2-}}{1\ mmol\ Cu^{2+}} * \frac{96.06\ mg\ SO_4^{2-}}{mmol} = 75.58\frac{mg}{L}\ SO_4^{2-}$$

Total sulfate concentration required:

$$\Delta S = \Delta S_{Zn} + \Delta S_{Cu} = 146.9\ \frac{mg}{L}\ + 75.58\ \frac{mg}{L}\ = \boldsymbol{222.5\frac{mg}{L}\ SO_4^{2-}}$$

# 11. Appendix E: Sulfate-Reduction Model Residuals

Determining the optimal fit of the sulfate-reduction model to experimental reactor performance data at 5°C and 22°C required a sum of least squares analysis using initial ages of 0.3, 0.5, 1 and 1.5 years and resultant sulfate reduction rate coefficients. Table XVI and Table XVII show the sum of least squares residuals corresponding to changes in initial age inputs while conducting the sum of least squares analysis of 22°C and 5°C operating conditions.

**Table XVI: Sulfate-reduction model sum of least squares residuals at various initial ages fit to 22°C reactor operation ($k_s$ = 0.581).**

| Initial Age | Residuals |
|---|---|
| **0.3** | -4,125,622 |
| **0.5** | $5.39 \times 10^{-9}$ |
| **1.0** | 2,286,766 |
| **1.5** | 2,630,768 |

**Table XVII: Sulfate-reduction model sum of least squares residuals at various initial ages fit to 5°C reactor operation ($k_s$ = 0.295).**

| Initial Age | Residuals |
|---|---|
| **0.3** | -53,776 |
| **0.5** | $9.12 \times 10^{-8}$ |
| **1.0** | 66,037 |
| **1.5** | 92,543 |

## SIGNATURE PAGE

This is to certify that the thesis prepared by Katrina Moreira entitled "Design Improvements to Sulfate-Reducing Bioreactors for Mine-Influenced Stream Remediation in Cold Climates" has been examined and approved for acceptance by the Department of Environmental Engineering, Montana Tech of The University of Montana, on this 10th day of April, 2018.

Raja Nagisetty, PhD, Assistant Professor
Department of Environmental Engineering
Chair, Examination Committee

Christopher Gammons, PhD, Professor
Department of Geological Engineering
Member, Examination Committee

Jeanne Larson, MS, Lab Director/Instructor
Department of Environmental Engineering
Member, Examination Committee

Robert Roll, MS, Senior Environmental Project Officer
Montana Department of Environmental Quality, State Superfund Section
Member, Examination Committee

William Drury, PhD, Professor, Retired
Department of Environmental Engineering
Member, Examination Committee